



Review

Cite this article: Marciello M, Pellico J, Fernandez-Barahona I, Herranz F, Ruiz-Cabello J, Filice M. 2016 Recent advances in the preparation and application of multifunctional iron oxide and liposome-based nanosystems for multimodal diagnosis and therapy.

Interface Focus **6**: 20160055.

<http://dx.doi.org/10.1098/rsfs.2016.0055>

One contribution of 12 to a theme issue 'Multifunctional nanostructures for diagnosis and therapy of diseases'.

Subject Areas:

bioengineering, nanotechnology, biomedical engineering

Keywords:

multimodal imaging, liposome, PET/MRI, molecular imaging, theranosis, iron oxide nanoparticles

Author for correspondence:

Marco Filice

e-mail: marco.filice@cnic.es

Recent advances in the preparation and application of multifunctional iron oxide and liposome-based nanosystems for multimodal diagnosis and therapy

Marzia Marciello¹, Juan Pellico², Irene Fernandez-Barahona², Fernando Herranz^{2,3}, Jesus Ruiz-Cabello^{2,4} and Marco Filice²

¹Department of Biomaterials and Bioinspired Material, Materials Science Institute of Madrid (ICMM-CSIC), Sor Juana Inés de la Cruz 3, Cantoblanco, Madrid, Spain

²Advanced Imaging Unit, Fundación Centro Nacional de Investigaciones Cardiovasculares Carlos III (CNIC), CIBER de Enfermedades Respiratorias, C/Melchor Fernández-Almagro 3, 28029 Madrid, Spain

³Departamento de Bioingeniería e Ingeniería Aeroespacial, Universidad Carlos III de Madrid, Madrid, Spain

⁴Universidad Complutense de Madrid, Plaza Ramón y Cajal, 28040 Madrid, Spain

MF, 0000-0001-8142-4566

Nowadays, thanks to the successful discoveries in the biomedical field achieved in the last two decades, a deeper understanding about the complexity of mechanistic aspects of different pathological processes has been obtained. As a consequence, even the standard therapeutic protocols have undergone a vast redesign. In fact, the awareness about the necessity to progress towards a combined multitherapy in order to potentially increase the final healing chances has become a reality. One of the crucial elements of this novel approach is that large amounts of detailed information are highly needed and *in vivo* imaging techniques represent one of the most powerful tools to visualize and monitor the pathological state of the patient. To this scope, due to their unique features, nanostructured materials have emerged as attractive elements for the development of multifunctional tools for diagnosis and therapy. Hence, in this review, the most recent and relevant advances achieved by applying multifunctional nanostructures in multimodal theranosis of different diseases will be discussed. In more detail, the preparation and application of single multifunctional nano-radiotracers based on iron oxides and enabling PET/MRI dual imaging will be firstly detailed. After that, especially considering their highly promising clinical potential, the preparation and application of multifunctional liposomes useful for multimodal imaging and therapy will be reviewed. In both cases, a special focus will be set on the application of such a multifunctional nanocarriers in cancer as well as cardiovascular diseases.

1. Introduction

Nowadays, as a consequence of the brilliant progress in biomedical technology achieved in the past decades, it is undoubtedly clear that the heterogeneity of the disease and patients is one of the most crucial factors impacting on the final favourable evolution of a pathological process. In other terms, there is no panacea and each patient needs optimized therapy based on the differences in genetic factors, physical conditions, environmental factors and the disease characteristics (personalized medicine) [1–3]. In this novel concept, large amounts of detailed information about the disease and patients are much needed. With this aim, non-invasive diagnosis of patients, *in vivo* imaging techniques result in one of the most powerful tools to visualize the pathological state of the body and monitor biological evolution at the target site [4].

For clinical application, the most useful imaging modalities generally include optical imaging, magnetic resonance imaging (MRI), computed tomography (CT), ultrasound (US) and positron emission tomography (PET) or single

photon emission computed tomography. Each single imaging modality shows unique advantages along with intrinsic limitations, such as insufficient sensitivity or spatial resolution. This circumstance makes it difficult getting accurate and reliable information at the disease site [5]. In order to improve the final diagnostic image and to characterize and quantify biological processes at the cellular and subcellular level in intact living subjects, the above-cited imaging modalities require the use of small molecules as probes (molecular imaging) [5]. For example, gadolinium complexes or iodinated compounds are used as contrast agents for T_1 -MRI or CT imaging, respectively. However, if not properly engineered, these small molecules generally present different limitations such as very short blood circulation time and non-specific biodistribution, which may cause many unwanted side effects.

In order to overcome many of these limitations, nanostructured materials can be employed [6]. In fact, it is a well-established reality the tremendous impact that nanotechnology development has had on society and especially in medicine. By virtue of their size-dependent physical properties and nanometre-scale dimensions, nanomaterials possess enormous synthetic design potential along with the ability to access biological features at the subcellular level. Hence, nanomaterials can be easily combined for multiple targeting, sensing, diagnostic and therapeutic functions [7]. This higher level of functional sophistication (not possible with small molecules) is the major driver for the development of nanomedicine, one of the fastest growing areas in nanotechnology and poised to revolutionize healthcare and medicine through the development of transformative new diagnostic and therapeutic tools [8].

The result of such a rational combination of different nanomaterials will then generate a novel multifunctional nanocarrier showing the best characteristic of their parental constituents and reducing their intrinsic limitations. In this way, different imaging and therapeutic strategies may be promoted at the same time (multimodal strategy), enhancing the final theranostic (therapeutic + diagnostic) effect. For example, the combination of MRI contrast agent and fluorescent organic dye on the same targeted nanocarrier allows detecting cancer through non-invasive MRI and the optical guide of surgery. Or, the encapsulation of MRI contrast agent and anti-cancer drug in a nanostructured matrix modified with a specific peptide or antibody on its surface has the potential to allow for simultaneous targeted diagnosis and chemotherapy [9].

One of the most notable consequences related to the advent of these multifunctional nanomaterials is the possibility of combining different imaging modalities with a unique contrast agent. Starting from its early dawn, multimodal imaging was revealed to be a powerful methodology able to provide more accurate detection and analysis of disease sites [8,10,11]. For example, the combination of PET with CT or MRI techniques has generated a strong interest due to the highly synergistic improvement of currently used imaging instruments for diagnosis. In fact, PET images provide functional information about the disease with high sensitivity. On the other hand, CT and MRI offer high-resolution images for anatomical information. Therefore, a combination of these different imaging modalities can accomplish high sensitivity and high resolution simultaneously and provide more detailed anatomical or biological information about the target disease. The theoretical combinations to produce multifunctional probes for multimodal

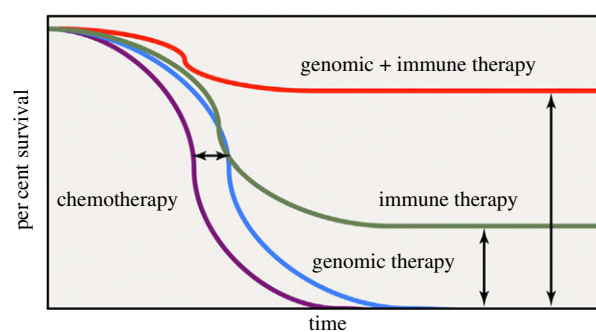


Figure 1. Improved overall cancer survival as a result of combination therapy. Adapted from [14].

imaging are directly related to the engineered nanomaterials reported until now. Consequently, such combinations could be considered unlimited [8,9,12,13]. Nevertheless, from a practical point of view, these combinations are limited in number because they finally must provide more precise and detailed information for clear diagnosis than the constituting individual modality. For this reason, the rational selection of each modality enabling the multimodal strategy is crucial. In this sense, researchers should rationally avoid the overlapping of advantages and compensate for the flaws of each selected strategy in order to maximize the synergistic effect. This is the reason why imaging modalities with high sensitivity (PET, optical, etc.) are frequently combined with other imaging modalities with high spatial resolution (MR, CT, etc.) [5,8,9].

Even from a therapeutic point of view, in parallel to the growing knowledge of the complexity of each pathological process, the awareness about the necessity to progress towards a combined multitherapy in order to potentially increase the final healing chances has become a reality. Combined therapy of two or more strategies promotes synergism among each individual constituent and targets the pathology through distinct mechanisms of action (figure 1). Within the different clinical applications where this rational concept has been successfully applied (i.e. antiviral and antimicrobial therapies), cancer therapy represents one of the clearest examples. In fact, dating from its early successful evidences, immunotherapy quickly became the fifth pillar of cancer treatment together with the well-known more traditional options including radiation, surgery, chemotherapy and targeted therapy (figure 2a) [14]. Scientists have shown repeatedly that using just one therapeutic modality, poor results would be achieved. Only combination of the above-mentioned modalities will produce a sustained and lasting response in a wider number of patients. No pillar alone holds up the architrave to keep the temple intact (figure 2a).

Even for the treatment of cardiovascular diseases (CVDs), the multitherapy approach has demonstrated its high potential. In fact, in the past decade, a multiactive all-in-one pill (polypill) composed of four drugs (aspirin, a cholesterol lowering statin and two blood pressure drugs (ACE inhibitor and a diuretic) that are known to effectively treat CVD) has been proposed as a simple, cost-effective and innovative public health strategy to combat the CVD epidemic on a global scale (figure 2b). Several randomized clinical trials have consistently demonstrated the effects of polypills on cardiovascular risk factors [15]. Moreover, besides the clinical potential, several other studies have shown the polypill to be well tolerated and superior in terms of patients' adherence to standard of care [15–17].

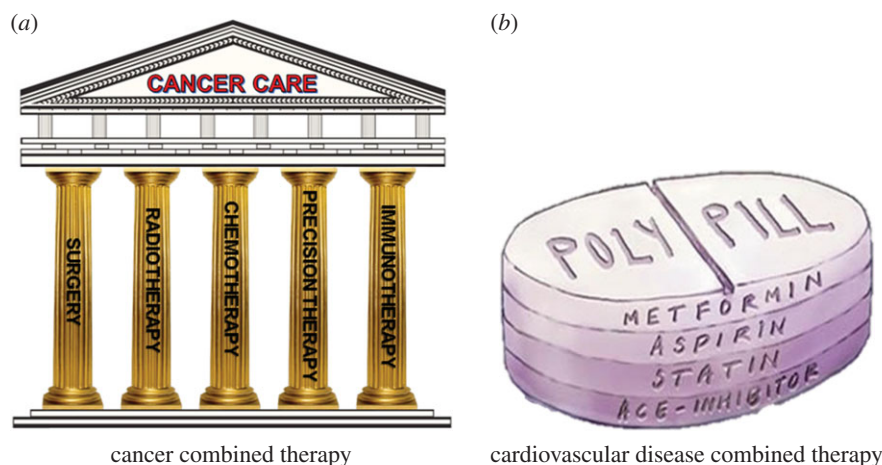


Figure 2. Schematic of combined multitier therapy in (a) cancer disease and (b) cardiovascular disease.

In the literature, countless examples of novel engineered nanomaterials with biomedical potential in human health have been published [13,17–19]. However, the vast majority of existing reviews tend to focus only on a specific application of nanomaterials in biomedicine (one therapeutic strategy or one imaging technique). Only some of them target the multimodal theranostic activity of composed nanosystems in different pathological processes. For this reason, in the present review, more detailed insights concerning the most recent and relevant achievements obtained by applying the multifunctional nanostructures in multimodal theranosis of different diseases will be discussed. This special focus has been carefully selected considering the highly promising results obtained to date by the combined use of different engineered smart nanomaterials in multimodal theranosis (synergistic effect) if compared with the same results achieved when the same nanomaterials were used individually (additive effect). Beside this aspect, among the plethora of existing nanosystems described in the literature, the focus will be set on the most promising ones in multimodal imaging as much as in multitier therapy of cancer and CVDs [20].

In more detail, as a representative example of a single multifunctional nanoprobe promoting multimodal imaging, the preparation and application of hybrid nano-radiotracers enabling the PET/MRI dual imaging of different pathological processes will be described. This particular theme was selected considering the rapidly growing interest in clinical application of such a multimodal imaging strategy. The different strategies enabling the preparation of these nanocarriers and their application in cancer and cardiovascular imaging and therapy will be discussed.

Subsequently, as a representative example of most promising nanomaterials useful in multimodal theranosis, the preparation and application of multifunctional liposomes will be reviewed. Indeed, within all the studied nanomaterials, these nanocarriers are the most used in clinical trials, showing the most promising commercial and clinical potential [20]. For example, in this direction, very recently a liposome-based system has been used to delivery RNA in three human patients with melanoma. As final result, a systemic immune response targeting melanoma cancer cells was triggered [21].

2. Nano-radiochemistry for multimodal imaging

The novel field of nano-radiochemistry tries to conjoin the best attributes of two branches of science that, in spite of all

their common features, have traditionally ignored each other. The combination of the size-dependent properties of nanomaterials and the exquisite sensitivity of nuclear techniques is creating a new paradigm in molecular imaging. These new features extend to most of the typical issues when developing tracers for biomedical imaging like the concept of multifunctionality, biodistribution, pharmacokinetics and the administered dose.

High surface/volume ratio is a well-known characteristic in almost all nanomaterials. This feature is particularly suitable for its conjugation with multiple molecules that provide multifunctionality. Apart from enabling bimodal imaging experiments, combination of nanomaterials with a radioisotope allows to obtain larger ligand payload in further bioconjugations, when compared with the common radiotracers, due to the multifunctionality of nanomaterials [22,23].

As previously stated, one critical issue related to the use of nanomaterials is their biodistribution. In fact, the biodistribution study of the nanomaterials is sometimes complicated and is frequently performed through *ex vivo* techniques using highly sensitive techniques [24,25]. In such a case, radiochemistry can clearly lend a hand to nanotechnology. By incorporating a radioisotope within the structural framework of the nanomaterial, the biodistribution can be studied effortlessly with *in vivo* and/or *ex vivo* radioactive techniques [26–30].

On the other hand, in the case of nano-radiotracers, nanotechnology comes to the aid of radiochemistry. From the point of view of pharmacokinetics, radiotracers sometimes present short circulation time in blood. To this scope, there are different strategies to improve the *in vivo* behaviour of radiotracers. One of the most used solutions is the attachment of PEGylated chains [31,32]. Even though PEGylated radiotracers usually show longer circulation times, this methodology needs at least one additional step, which increases synthetic cost and time. A clever solution to increase circulation time of the tracer is to incorporate it into a nanoplatform with an intrinsic long circulation time in blood [33,34]. Nano-radiochemistry also benefits from the possibility of including specific ligands on the surface of nanoparticles in order to direct nanoplatforms to desired sites, increasing specificity and efficiency of radiotracers.

Furthermore, the possibility of combining not only one, but several labels for different imaging modalities allows signal amplification. This special feature combined with high sensitivity of nuclear techniques and enhanced surface area presented by

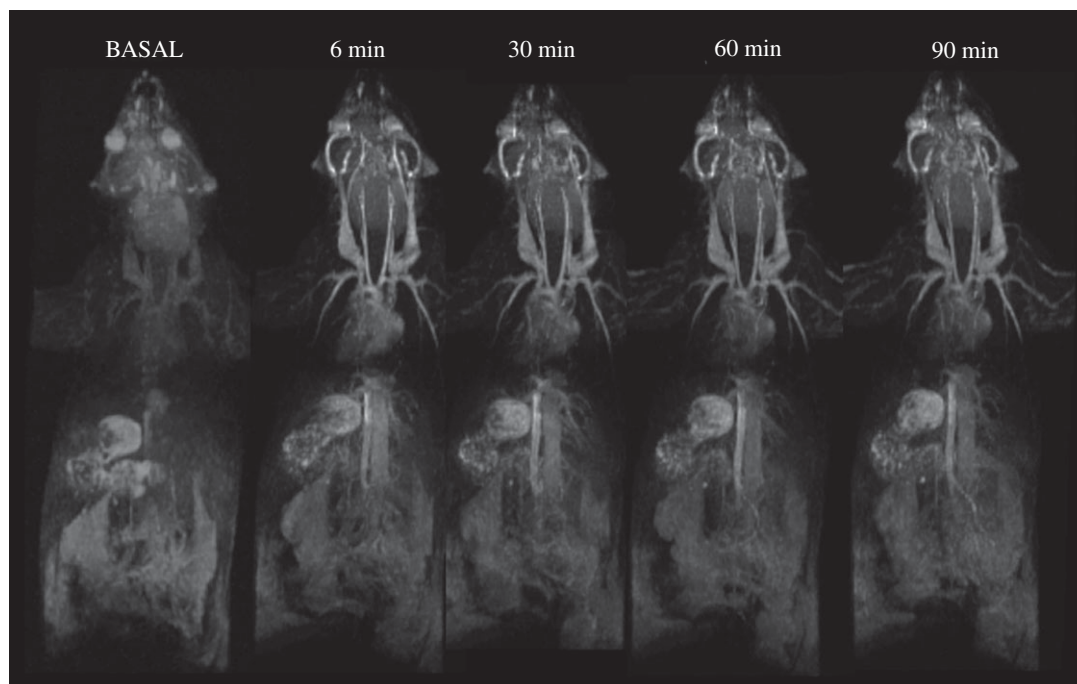


Figure 3. Magnetic resonance angiography of a mouse at increasing times after intravenous injection of fdIONP. Adapted from [42].

nanoparticles allows significant dosage reduction if compared with the single modality acquisition strategy.

2.1. Iron oxide nanoparticles for imaging

Iron oxide nanoparticles (IONPs) are the most common NP-based contrast agent for MRI [35]. MRI offers excellent soft-tissue contrast resolution and pathological discrimination. On the other hand, PET, one of the most typical molecular imaging techniques, presents poor probe anatomical localization potential [36]. Consequently, the fusion of these two techniques in a single measurement (PET/MRI) may help to overcome in some applications the lack of anatomical details offered by PET and poor sensitivity of MRI. IONPs have for long been studied as MRI probes for T_2 -weighted (dark or negative contrast) imaging. The T_2 (the transverse relaxation time) based contrast from these IONPs is an intrinsic effect of their crystalline core and high magnetic moment. As an effect, they finally damp the signal of the nearby water molecules. The list of researches focusing upon this nanocarrier is enormous [11,13,37–41]. The interest normally lies in the improvement of the core crystal or surface functional structure, so as to make it as biocompatible as possible, while modifying the surface so as to enhance the target specificity to the maximum.

However, this marked effect on T_2 can be a problem for many imaging applications. For example, it is crucial when the signal intensity is intrinsically low due to physiological and magnetic susceptibility characteristics of the organ/tissue (lungs, trabecular bone, paranasal sinus, etc.) or due to the presence of low-proton contents (necrosis, calcifications, etc.) in some pathologies. In these cases, the large negative contrast promoted by superparamagnetic iron oxide is not the best option. Because of that, in the last years there has been an intense development of extremely small (2–3 nm core size), superparamagnetic, IONPs as T_1 contrast agents [42,43]. In this case, the effect observed here is the shortening of longitudinal relaxation time (T_1). This T_1 -based (bright or

positive) contrast is usually of more practical use for physicians when compared with its T_2 counterpart. In one of our works, we illustrated this possibility using a microwave assisted one-pot synthesis of extremely small, FITC-CM dextran (4 kDa) capped iron oxide nanoparticles (fdIONP) for T_1 -based MRI contrast [42]. The particles were biocompatible, showed a long circulatory half-life and multimodal imaging ability due to the presence of FITC, especially for histological validation (figure 3) [11].

2.2. Nano-radiolabelling

2.2.1. Radioisotopes

There are many different radioisotopes that may be used as positron emitters in PET. They are usually classified according to their half-life time or production method. In the case of the half-life time, there are a large variety of radioisotopes covering all range spectra (table 1). Isotopes range from a very short half-life time like ^{15}O (approx. 2 min) to long half-life time like ^{124}I (4.18 days). Moreover, this half-life time of the radioisotope will determine its use in PET imaging. For long-time elimination tracers, the use of short half-life time radioisotopes is preferable for clinical purposes in order to reduce the patient's radioactivity exposure [44]. Despite this, sometimes there is no choice and a long half-life radioisotope has to be used, for instance, to visualize biological molecules with long circulation time in blood. Radioisotopes are commonly produced in a cyclotron (particle accelerator). This fact represents a disadvantage for radioisotopes with short half-life time due to the necessity of having a cyclotron close to the PET camera. Moreover, cyclotrons are expensive and require specific facilities. Another production method is through benchtop generators. These are portable armoured cylinders that contain a matrix with a father radioisotope embedded. Generators are small, usually cheap and easy to use, which is the main advantage of this methodology [45]. However, the use of generators for PET radioisotopes is limited to only two elements, ^{68}Ga and ^{32}Rb .

Table 1. Main radioisotopes for molecular imaging.

radioisotope	half-life	units	production route
^{11}C	20.4	minutes	$^{14}\text{N}(\text{p},\alpha)^{11}\text{C}$ (cyclotron)
^{13}N	9.9	minutes	$^{14}\text{O}(\text{p},\alpha)^{13}\text{N}$ (cyclotron)
^{15}O	122	seconds	$^{14}\text{N}(\text{d},\text{n})^{15}\text{O}$ (cyclotron)
^{18}F	110	minutes	$^{18}\text{O}(\text{p},\text{n})^{18}\text{F}$ (cyclotron)
^{62}Cu	9.74	minutes	$^{63}\text{Cu}(\text{p},\text{n})^{62}\text{Cu}$ (cyclotron) $^{62}\text{Zn} \rightarrow ^{62}\text{Cu}$ (generator)
^{64}Cu	12.7	hours	$^{64}\text{Ni}(\text{p},\text{n})^{64}\text{Cu}$ (cyclotron) $\text{Zn}(\text{various})^{64}\text{Cu}$ (cyclotron)
^{68}Ga	67.7	minutes	$^{69}\text{Ga}(\text{p},2\text{n})^{68}\text{Ge}$ (cyclotron) $^{68}\text{Ge} \rightarrow ^{68}\text{Ga}$ (generator)
^{76}Br	16.2	hours	$^{76}\text{Se}(\text{p},\text{n})^{76}\text{Br}$ (cyclotron)
^{124}I	4.15	days	$^{124}\text{Te}(\text{p},\text{n})^{124}\text{I}$ (cyclotron)
^{89}Zr	78.4	hours	$^{89}\text{Y}(\text{p},\text{n})^{89}\text{Zr}$ (cyclotron)
^{82}Rb	76	seconds	$^{82}\text{Sr} \rightarrow ^{82}\text{Rb}$ (generator)

Because of its matched half-life for tagging many biological processes and production method in a generator, ^{68}Ga is becoming an extremely important radioisotope in radiochemistry [46,47]. These generators contain a matrix with father isotope ^{68}Ge that present a long half-life of 270 days allowing the elution of ^{68}Ga for months, with the same generator. Half-life of ^{68}Ga (67.7 min) is similar to circulation time in blood of many peptides, which makes this radioisotope very attractive for their *in vivo* visualization. There are some examples of the synthesis of ^{68}Ga -based radiotracers. For example, within the most used radiotracers to assess somatostatin receptors, ^{68}Ga -DOTATATE and ^{68}Ga -DOTATOC were introduced for their high specificity towards different neuroendocrine tumours [48–50].

2.2.2. Radiolabelling of iron oxide nanoparticles: nano-radiochemistry

Different strategies for the synthesis of nano-radiotracers based on IONPs are available. The principal difference concerns the localization of the radioisotope with respect to the nanoparticle structure. In the first case, the radioisotope is tagged within the surfactant of the nanoparticle and, therefore, this approach is called surface labelling. The second option comprises doping the core of the nanoparticle with the radioisotope and is called core labelling. Both methods have some advantages and disadvantages that will be summarized in the following paragraphs.

2.2.3. Surface labelling

One of the most important features of nanoparticles is the high surface/volume ratio. This intrinsic characteristic provides the capability of multifunctionalization in the surface of the nanoparticle [51,52]. Surface labelling takes the advantage of this specific surface for the conjugation of the nanoparticle with the radioisotope.

2.2.3.1. Chelator strategy

A common way to produce the nano-radiotracer is to functionalize the nanoparticle with a chelate ligand, in order to

form a coordination complex between the nanoparticle and the radioisotope in a final step.

Despite its easiness, there are two different important issues that must be taken into account with this approach. The first one is the stability of the bond between the nanoparticle and the chelator agent, and the second is the stability of the coordination complex between the chelator and the radioisotope.

Concerning the first aspect, a strong covalent bond between the nanoparticle and the chelator is preferred so as to avoid *in vivo* desorption. In PET imaging, the signal derives from the radioisotope. If the chelator is desorbed from the surface of the nanoparticle, the signal of the radioisotope will come from the chelator-radioisotope coordination complex and not from the nano-radiotracer. Therefore, the use of organic chemistry to obtain stable chelate-functionalized nanoparticles is mandatory, with many different options depending on the desired final formulation.

The second important aspect to take into account regarding this approach is the stability of the coordination complex between the chelator and the radioisotope. Owing to the presence of different cations in blood, transmetalation reactions involving the nano-radiotracer can occur. To avoid this process, the use of high affinity complex between the chelator and the radioisotope is required. The choice of the radioisotope determines the chelator. A very common chelator in the ^{68}Ga radiolabelling of IONPs is 1,4,7,10-tetraazacyclododecane-1,4,7,10-tetraacetic acid, also known as DOTA. The use of a chelating agent to build the nano-radiotracer presents, in a general way, some advantages and disadvantages in comparison with other strategies. The main advantage in the use of a chelator on the surface of the nanoparticle is that it allows multifunctionalization of the nano-radiotracer before the radiolabelling step. However, this technique requires a multiple-step synthesis and purification protocol.

To overcome the necessity of a multiple-step synthesis, other methods have appeared, called chelator-free synthesis.

2.2.3.2. Chelator-free strategy

Chelator-free approaches are mainly based on the addition of the radioisotope directly over the surface of the nanoparticle without the use of a chelator. Only a few examples based on this strategy have been reported. For example, one of them exploits the affinity of the magnetite towards arsenic for the synthesis of radioarsenic-labelled IONPs [53]. The mechanism of the sorption of the arsenic onto IONPs is known and it has been used in contaminated anoxic groundwaters to reduce the toxicity [54]. Another example of this approach is the synthesis of ^{69}Ge radiolabelled IONPs. The incorporation of another germanium radioisotope such as ^{68}Ge onto metal oxides is well known and it has been long used for the fabrication of $^{68}\text{Ge}/^{68}\text{Ga}$ generators [55,56]. In this case, the authors took the same idea as previously described in studies with ^{68}Ge , to incorporate ^{69}Ge directly on the surface of the nanoparticle without the help of chelators [57].

Albeit these methods are adequate for the radiolabelling of IONPs, there are some inherent drawbacks. Firstly, desorption of the radioisotope could be a problem for *in vivo* behaviour giving a low signal/noise ratio or toxicity problems when using isotopes like arsenic. Moreover, the existing methods are limited to radioisotopes without translational potential, which is the main disadvantage of the strategy.

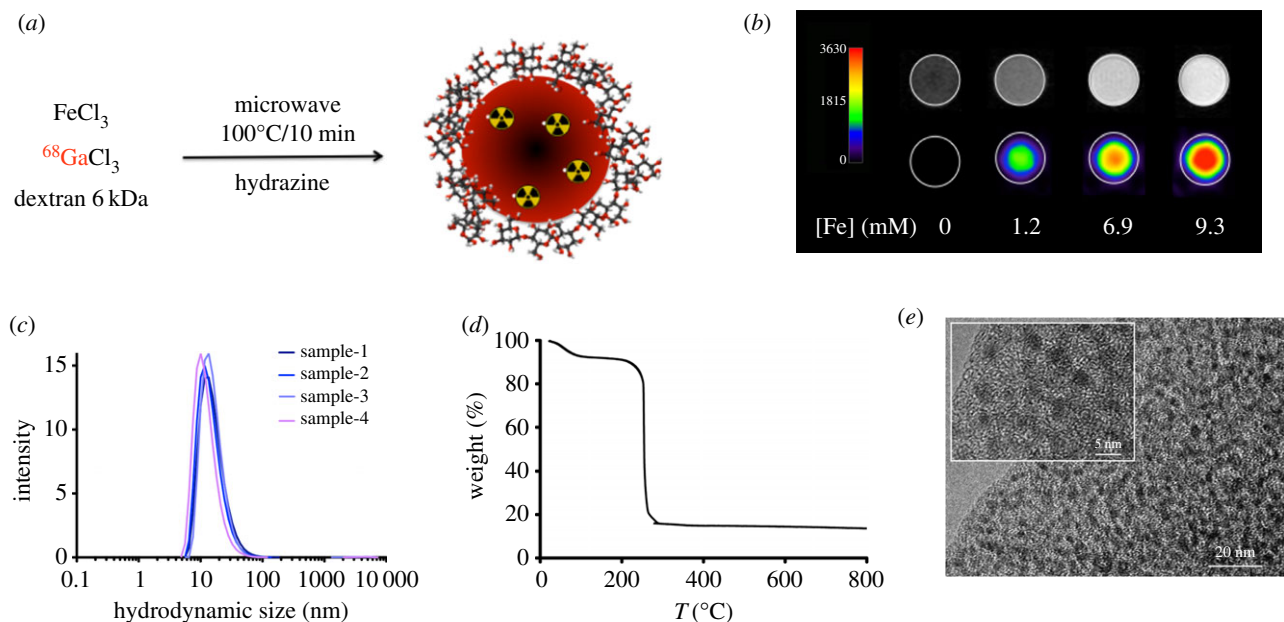


Figure 4. (a) Synthesis of ^{68}Ga core-doped IONPs; (b) image phantoms obtained at different iron concentrations by MRI (top row) and PET (bottom row); (c) hydrodynamic size of four different samples of ^{68}Ga core-doped IONPs; (d) thermogravimetric curve of ^{68}Ga core-doped IONPs and (e) TEM images of the sample. Adapted from [64].

2.2.4. Core labelling

Core labelling methodology is the newest approach for the production of chelator-free nano-radiotracers. This synthetic strategy combines non-radioactive precursor materials and a radioactive material to dope the core simultaneously with nanoparticle formation.

Hence, under appropriate conditions the radioisotope is entrapped inside the crystalline structure of the nanoparticle. Consequently, the location of the radioisotope (inside the core) ensures radiochemical stability, avoiding desorption or transmetallation reactions, making this approach very attractive, particularly in combination with isotopes of short half-life such as ^{68}Ga . In fact, when the nanoparticle core starts to be degraded *in vivo*, the radioactivity has been long decayed.

Owing to the novelty of the method, as far as we know, there are only two examples of core-labelled IONPs described in the literature. Both of them expect microwave technology to be driving force of the synthesis. The reason why microwave technology is important in the process, lies in the reaction rate. Synthesis of IONPs by traditional methods like co-precipitation or thermal decomposition of organic precursors lasts from 3 to 24 h [58,59]. Common reaction times are unsuitable when a radioactive material is used as initial reagent. Microwave technology uses dielectric heating and can produce high-quality IONPs in shorter times, more adequate for this strategy [60–62]. Moreover, microwave technology provides synthetic methods with high reproducibility.

The first example of core-doped iron oxide nanoparticles was described in 2012 by Wong *et al.* [63]. In this work, the authors described a microwave-driven synthesis of IONPs doped with ^{64}Cu . In this case, the radiolabelling yield was modest (33%) giving a low specific activity [63].

Very recently, our group described the synthesis of IONPs doped with a short half-life radioisotope such as ^{68}Ga with microwave the driving force of the reaction (figure 4a). In 15 min overall time, our protocol retrieved ^{68}Ga core-doped nanoparticles with very large radiolabelling yield (93%) and specific activity (7.6 GBq/mmol Fe).

Furthermore, the particles showed large r_1 value, which enables their use as T_1 -weighted (positive) contrast agents for MRI. This was the first example of the combination of IONPs for PET/(T_1) MRI (figure 4b). One of the key aspects on this approach is the reproducibility (figure 4c) and the thick organic layer (figure 4d) that guarantees very good colloidal stability and large number of functional groups for further functionalization for such extremely small nanoparticles of 2.5 nm core size (figure 4e).

2.3. Applications of iron oxide nanoparticles as multimodal imaging probes

2.3.1. Nanotechnology for cancer

In the past two decades, there have been countless discoveries regarding molecular bases of cancer; however, very few of them endure the vigorous clinical trials they must undergo in order to become useful in clinics [65]. Furthermore, there is still an absence of implementations to directly study molecular events in depth. For this reason, attention of oncologists and researchers is drawn to the development of novel approaches and techniques to improve outcomes [66,67]. Nanotechnology, as an interdisciplinary field involving biology, chemistry, engineering, medicine and physics, offers a wide variety of advantages in cancer diagnosis and therapy [34,68–70]. Multimodal therapy, early diagnosis and image-guided surgery or therapy are some examples of the same [66,71].

In this direction, IONPs have been widely used as MRI contrast agents as well as an excellent platform to which radionuclides can be incorporated, finally enabling an engineered molecular probe for dual imaging.

For example, radiolabelled poly(aspartic acid)-coated and PLGA-coated IONPs were used in two different studies for PET/MRI scanner of tumour integrin $\alpha_v\beta_3$ expression [72,73]. IONPs were coupled to RGD peptide and DOTA chelator prior to labelling with ^{64}Cu . The probe was proved to be tumour-specific by both PET and MRI.

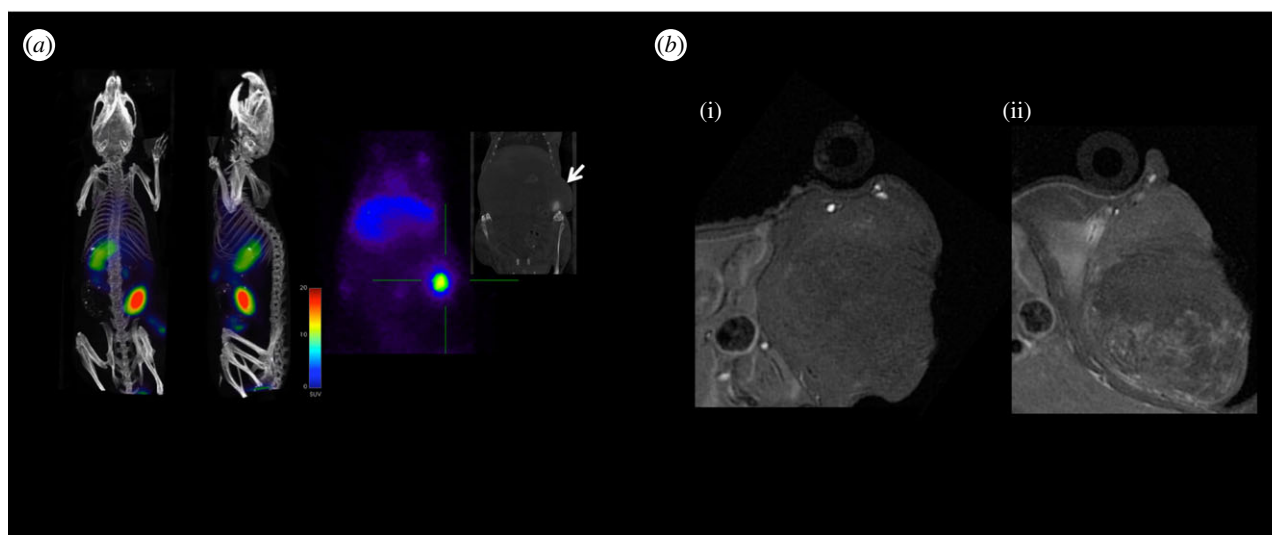


Figure 5. (a) PET/CT imaging of tumour-bearing mice 1 h post injection of ^{68}Ga -C-IONP showing activity in tumour. (b) Axial T_1 -weighted MRI of tumour area in a murine model previous to injection (i) and 24 h post injection of ^{68}Ga -C-IONP (ii). Adapted from [64].

Another example of IONP-based dual probes for PET/MRI is represented by ^{124}I -labelled IONPs. These nanoparticles were coated with serum albumin to secure high colloidal stability in a wide pH range and at high salt concentrations. They were used to track lymph nodes, crucial trademarks for cancer staging.

Likewise, Yang *et al.* [74] chose to monitor lymph node uptake of ^{68}Ga doped IONPs for T_2 -weighted MR imaging and PET. Multimodal mannose IONPs containing NOTA chelator were radiolabelled with ^{68}Ga . *In vivo* imaging showed these complexes could be specifically taken up by macrophages in lymph nodes.

Very recently, Pellico *et al.* reported the practical synthesis of chelator-free iron oxide-based nanotracers labelled with ^{68}Ga . In more detail, dextran-coated IONPs were core-doped with the radioisotope by a microwave-driven protocol, allowing an efficient and rapid synthesis [64]. These ^{68}Ga core-doped IONPs (^{68}Ga -C-IONP) were conjugated to RGD and assessed in an angiogenesis murine model. *In vivo* experiments confirm their specific accumulation in the tumour, by both PET and MRI. Figure 5 shows how the extremely high sensitivity of PET nicely matches the high resolution of MRI. Plus the core doping of the nanomaterial easily enables studying the biodistribution by gammacounter with sensitivity unparalleled by any other technique.

2.3.2. Nanotechnology for cardiovascular diseases

CVD encompasses all diseases concerning the heart and circulation, including atherosclerosis, coronary heart disease, angina, heart attack, congenital heart disease and stroke [75]. It is the leading cause of death globally and usually stems from vascular dysfunctions. Major advances in treating these diseases have taken place in the past few decades [76], mainly regarding early diagnosis in which new imaging approaches play a crucial role. Molecular imaging allows aiming at specific molecular targets, biological processes and certain cell types, providing a valuable insight into molecular and cellular mechanisms [77]. Nonetheless, molecular imaging requires extremely sensitive and specific agents which should include a signal detection compound and an affinity ligand which directs it to the intended site. As a result, nanoparticles have gained significant interest as

agents for cardiovascular imaging and therapy [78]. Nanoconjugates arise as platforms for multiple entity integration, including targeting ligands, therapeutic agents and contrast materials. Different kinds of NPs have been used for imaging and therapy of different CVD.

Ischaemic and infarction lesions have been monitored and treated with several radiolabelled polymeric conjugates in different studies. Polyethylene glycol/phosphatidyl-ethanolamine (PEG-PE). ^{111}In -labelled micelles were successfully used by Lukyanov *et al.* [79] to passively target infarcted myocardium in rabbit models, taking advantage of enhanced permeability and retention (EPR) effect. Radiolabelled lipoprotein-composed nanoparticles (LDL and HDL) have been used to monitor lipoprotein circulation and uptake in atherosclerotic lesions [80]. Other radiolabelled NP types such as dextran NPs, dendrimers and polymeric NPs have also been reported as agents for atherosclerosis detection. Their targeting at inflammatory cells has confirmed their virtue as effective agents for intraplaque inflammation detection and may allow targeted drug delivery and release to stabilize plaques before they rupture and originate severe vascular events. Examples of these are the ^{64}Cu -labelled dendrimers used by Seo *et al.* to target macrophages with LyP-1 cyclic peptide [81]. ^{64}Cu was also chosen by Luehmann *et al.* [82] to label comb-like polymer NPs targeted towards chemokine receptor 5 (CCR5), which has been reported to be an active participant in late stages of atherosclerosis.

IONPs have been reportedly used in a variety of CVDs. A multifunctional probe composed by dextran-coated cross-linked IONPs labelled with a near-infrared fluorochrome and ^{18}F radionuclide for PET has been studied as a blood pool contrast agent detectable by PET fluorescence molecular tomography and MR imaging [83].

Radiolabelled IONPs have also been used for inflammatory cell imaging. Dextran-coated cross-linked IONPs labelled with ^{64}Cu were used by Ueno *et al.* [84] to quantify myeloid cell infiltration in murine cardiac allografts. The same group previously used ^{18}F -labelled cross-linked IONPs to target macrophages and monocytes in a murine model of aortic aneurysm in order to determine its dimensional stability. Jung *et al.* [85] carried out a study to assess the capability of HDL conjugates to assess atherosclerotic lesions in murine models by multimodal

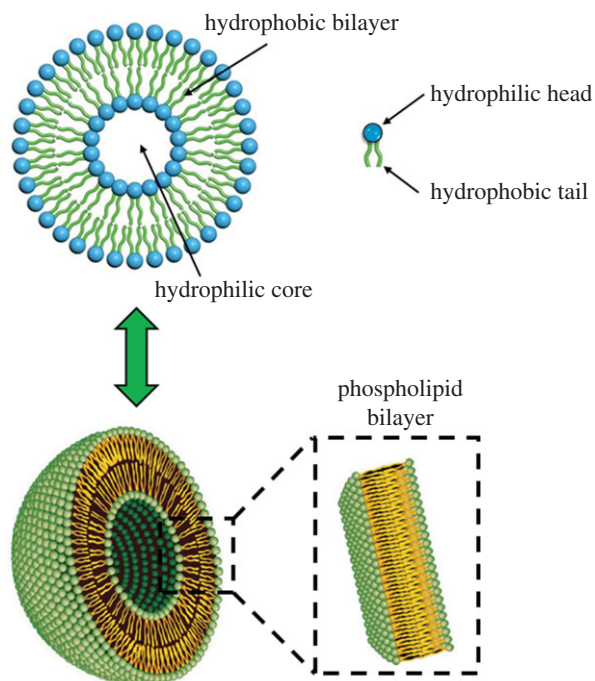


Figure 6. General scheme of liposomes. (Online version in colour.)

detection. Three different HDL-coated NPs were used for this purpose. Firstly, HDL-QD conjugates composed by Cd/Se/CdS/ZnS core-shell-shell and coated with HDL for optical imaging were obtained. A second probe, to be used as MRI contrast agent, was obtained using superparamagnetic IONP core and HDL coating (HDL-SPIO). The third probe type was composed of HDL-SPIO radiolabelled with ^{59}Fe , to be used in MRI and to detect radioactivity using a gamma counter. Biodistribution of these conjugates was studied using the different detection techniques. The similarities of HDL-NP conjugates with respect to endogenous HDL allowed quantification of radiolabelled complexes' accumulation in atherosclerotic plaques through MRI, X-ray fluorescence microscopy, confocal fluorescence microscopy and light microscopy.

3. Liposomes for multimodal theranosis

3.1. General properties of liposomes

Liposomes have gained large attention in the nanomedicine field for research and clinical applications [86,87]. They are vesicles consisting of amphiphilic phospholipids (e.g. phosphatidylcholine, phosphatidyl-ethanolamine, phosphatidylserine and phosphatidylglycerol) that form a lipid bilayer enclosing an aqueous core. Hence, they can encapsulate both hydrophobic and hydrophilic molecules that will be arranged in the opportune compartment (figure 6). This is an interesting advantage because biomolecules/drugs of different nature can be encapsulated together or alone in these interesting nanosystems depending on their characteristics. Other advantages of liposomes consist of degradation prevention of the incorporated biomolecule, reduction of drug toxicity with improved efficacy and therapeutic effect, versatility and biocompatibility [86,87].

Liposome surface can be functionalized to enhance the control of their pharmacokinetics and biodistribution. For example, polyethylene glycol (PEG) can be used to increase the nanosystem lifetime in the blood or targeting molecules can be anchored on the liposome surface promoting their directing

Table 2. Commercial liposome-based drug delivery systems.

product name	encapsulated drug	approved treatment
Myocet	doxorubicin	metastatic breast cancer [95]
Doxil	doxorubicin	Kaposi's sarcoma, ovarian and breast cancer [96–98]
Lipodox	doxorubicin	Kaposi's sarcoma, ovarian and breast cancer [99]
Marqibo	vincristine sulfate	acute lymphoblastic leukaemia [100]
DaunoXome	daunorubicin	blood tumours [101]
Epaxal	inactivated hepatitis A virus	hepatitis A [102]
DepoDur	morphine sulfate	pain management [103]
DepoCyt	cytarabine	neoplastic meningitis and lymphomatous meningitis [104]

to target cells. These allow the nanosystem to recognize the microenvironment and react in a dynamic way mimicking the response of living organisms and permitting the drug release at the selected place by time-controlled mechanism [88].

For all these reasons liposomes have been widely studied, overall as drug delivery systems, as reported in several reviews [86–94]. Moreover, they attracted the attention of pharmaceutical industries as demonstrated by the approval of several liposomal drug formulations for cancer therapies or other diseases (infections, pain, meningitis, hepatitis A, influenza, etc.; table 2). Besides the approved ones, other liposome formulations are undergoing clinical trials, more of them for cancer treatment [86]. Examples of liposome-based formulation that are actually in trial phase III for cancer treatment are represented by ThermoDox (for the release of doxorubicin in breast cancer) [105] and Lipoplatin (for the controlled release of cisplatin in pancreatic, breast, non-small cell lung, head and neck cancers) [106–110].

3.2. Methods of liposome preparation

Several methods reporting the preparation of liposomes with numerous variants have been reported [86,87]. On continuation, a description of the most common used methods for the development of these nanosystems will be briefly reviewed.

The easier and older method, described in 1965, is the Bangham method or thin lipid film hydration method [111]. It consists of the formation of a thin film of lipids after evaporation of organic solvents followed by freeze-drying to ensure solvents complete elimination. This film is then rehydrated by aqueous solvents. The molecules that must be incorporated inside the liposome can be solubilized in organic or aqueous medium depending on their nature. To reduce the size of the prepared liposomes (less than or equal to 200 nm) sonication, homogenization or extrusion methods are used, depending on the final desired size.

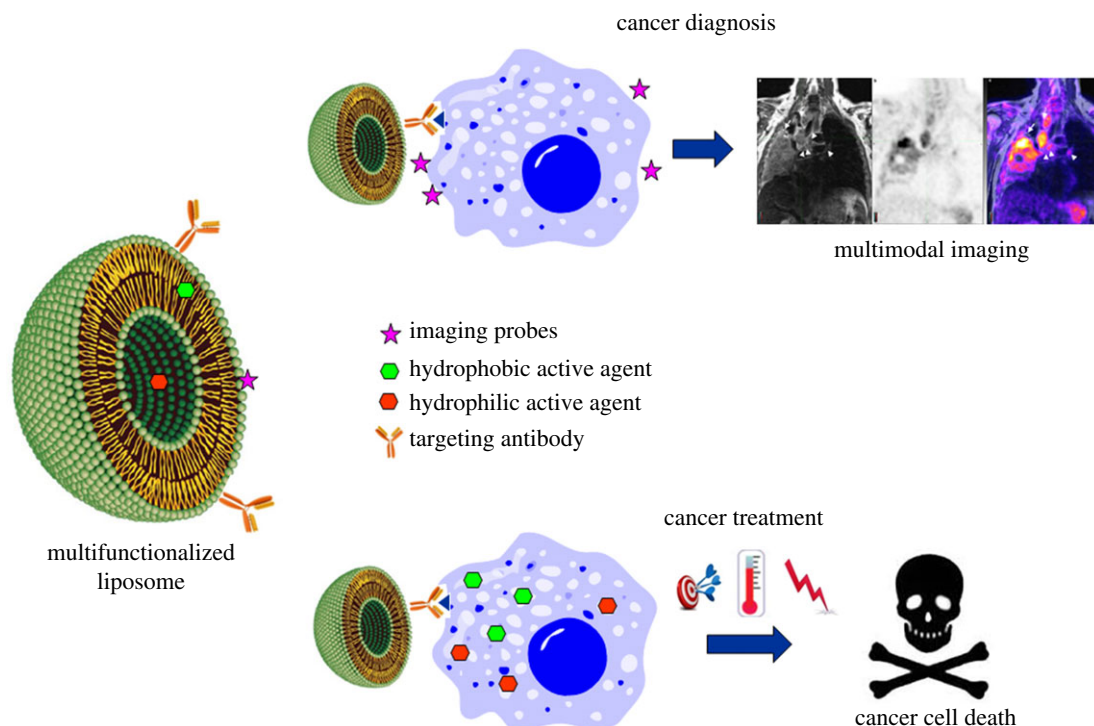


Figure 7. Schematic of multifunctionalized liposome and its application for cancer diagnosis and therapy.

An alternative method is the reverse phase evaporation technique. Inverted micelles or water-in-oil emulsions containing the molecule of interest in the aqueous phase and lipids composing the organic phase are initially formed [82,87]. The slow elimination of the organic solvent leads to the formation of liposomes. A higher internal aqueous loading with respect to the anterior method is obtained. The excess of solvent can be eliminated by dialysis, centrifugation or gel filtration [112].

Another method is the solvent injection technique. This is based on the injection of phospholipids dissolved in organic solvent (ethanol or ether) into an excess of aqueous solution containing the drug [113,114].

Also other novel methods for the preparation of liposomes such as double emulsion, freeze–thaw, dehydration–rehydration or fast-extrusion have been described [87]. For example, very recently, a technique based on the use of supercritical carbon dioxide has been developed [115].

3.3. Multifunctional liposomes

Besides their use as drug delivery systems, recently, the liposomes were considered in order to develop patient personalized therapies, to learn about genetic makeup of the subject and how the specific tumour is evolving [116–118]. By this way prevention, screening and treatment strategies should be more effective and the side effects reduced. Thus, the resistance problems associated with the use of a single therapeutic strategy, causing the failure of the treatment, can be overcome [119].

For this purpose, different strategies could be adopted. Nano-systems could be employed as theranostic agents or to induce multiactive therapies [117]. In the first case, tumour diagnosis and treatment can be obtained by the same formulation. With the second approach the disease can be monitored and fought by the synergistic effect of more than one therapy (figure 7).

Examples of multifunctionalized liposome preparation and application to obtain a personalized cancer therapy are reported in the following paragraphs.

3.3.1. Theranostic liposomes

MRI-guided drug delivery is a new approach to obtain a personalized therapy combining cancer diagnosis with therapy accompanied by monitoring of clinical response in real time.

A theranostic liposomal system for lung cancer including both hydrophilic (carboplatin) and hydrophobic (paclitaxel) drugs was designed by Ren *et al.* [120]. The imaging ability was assured by the presence of a T₁-contrast agent (gadodiamide) and a fluorescent molecule (rhodamine). The surface was functionalized with a targeting peptide (c(RGDyK)) specific for receptors overexpressed in many tumour cells. After liposome internalization by endocytosis, its payload was released enhancing diagnostic and therapeutic results. Hence, the cancer cells were firstly detected by MRI and confocal microscopy. Owing to the architecture of the system, it was proved that the tumour signal was enhanced in comparison with commercial contrast agent Omniscan[®] (figure 8), and liposome biodistribution *in vivo* imaged via T₁-weighted MRI in real time and simultaneous chemotherapeutic effect was shown [120].

In another work, an MRI-based theranostic liposome was developed for the diagnosis and treatment of breast cancer [121]. A hydrophobic chemotherapeutic drug (doxorubicin) and a hydrophilic contrast agent (gadoteridol) were co-encapsulated inside a liposome. This nanosystem was able to release its content into the tumour cells. Thanks to the presence of the contrast agent it was possible to visualize the doxorubicin release by MRI. The therapeutic efficacy of the drug was improved by two different techniques based on pulsed US. More in detail, the US waves acted at the same time as *stimuli* useful to trigger the drug release as well as *sonoporation stimulus* enhancing tumour vascular permeability to the drug. A marked increase of drug concentration in the cancer cells followed by a complete tumour regression was so obtained (figure 9).

Theranostic liposomes were also developed using T₂-weighted contrast agents such as magnetic nanoparticles

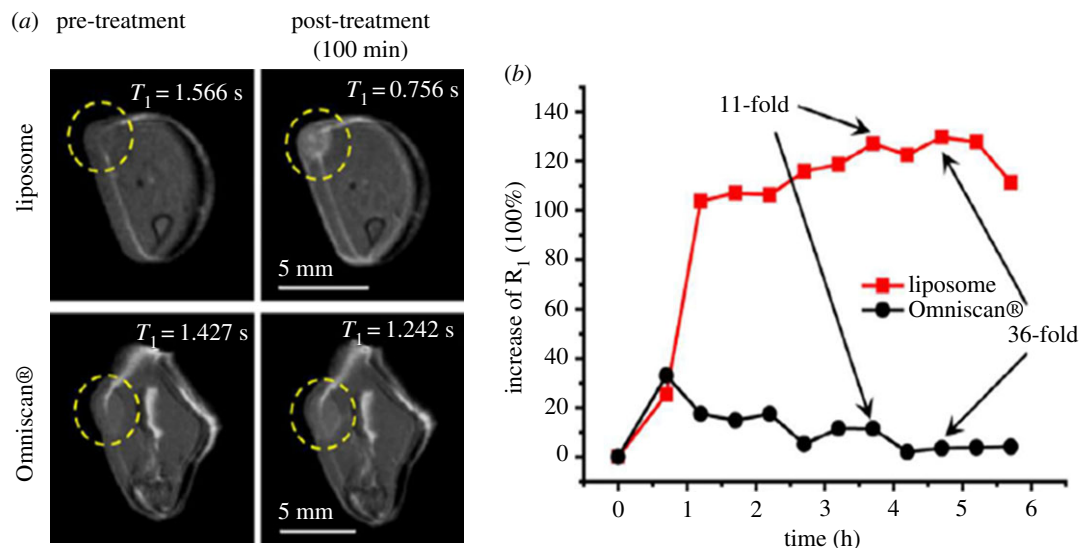


Figure 8. MRI analysis of the tumours after treatment with the developed multifunctionalized liposome compared with Omniscan®. (a) Increase of T_1 relaxation rate (R_1) over time. (b) R_1 was enhanced 11- and 36-fold, respectively, 3.7 h and 4.7 h after injection with respect the commercial formulation Omniscan®. Adapted from [120].

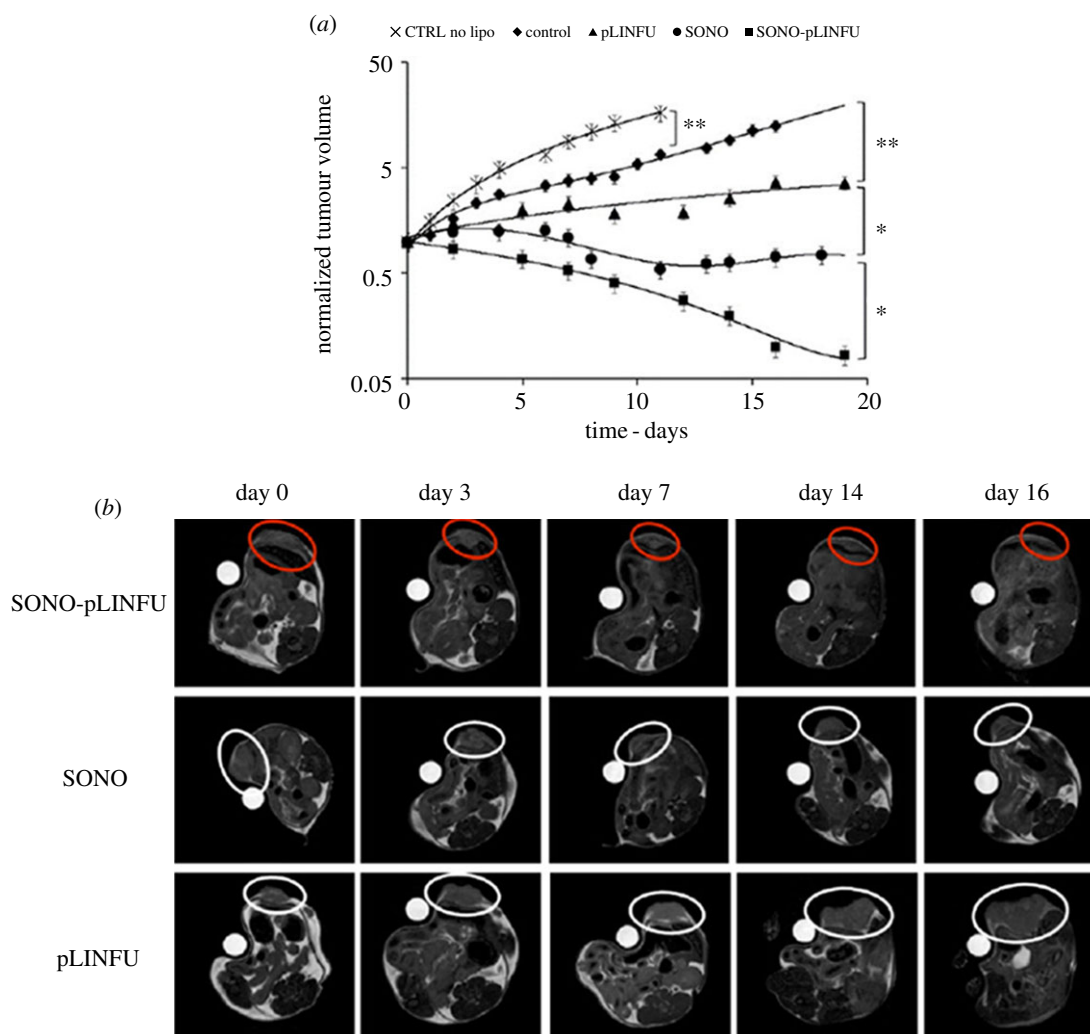


Figure 9. MRI images of (a) tumour progression; (b) US-treated mice. The images were acquired at the time of the first MRI session (day 0) and after 3, 7, 14 and 16 days. 'Sonoporation stimulus' (SONO) was applied during the liposome injection, while the 'release stimulus' (pLINFU) was applied just after sonoporation. CTRL no LIPO refers to a group of mice that was not injected with liposomes. Adapted from [121].

(MNPs). The unique property of magnetism of these particles allows an active targeting to the desired cells by using a permanent magnetic field. Carboxymethyl-dextran-coated magneto liposomes were hence prepared demonstrating

their utility in diagnostic/therapeutic efficacy for some cancers such as brain cancer. Doxorubicin and MNPs were loaded into liposomes and released at target cells through pH- and magnetic-dependent mechanisms [122].

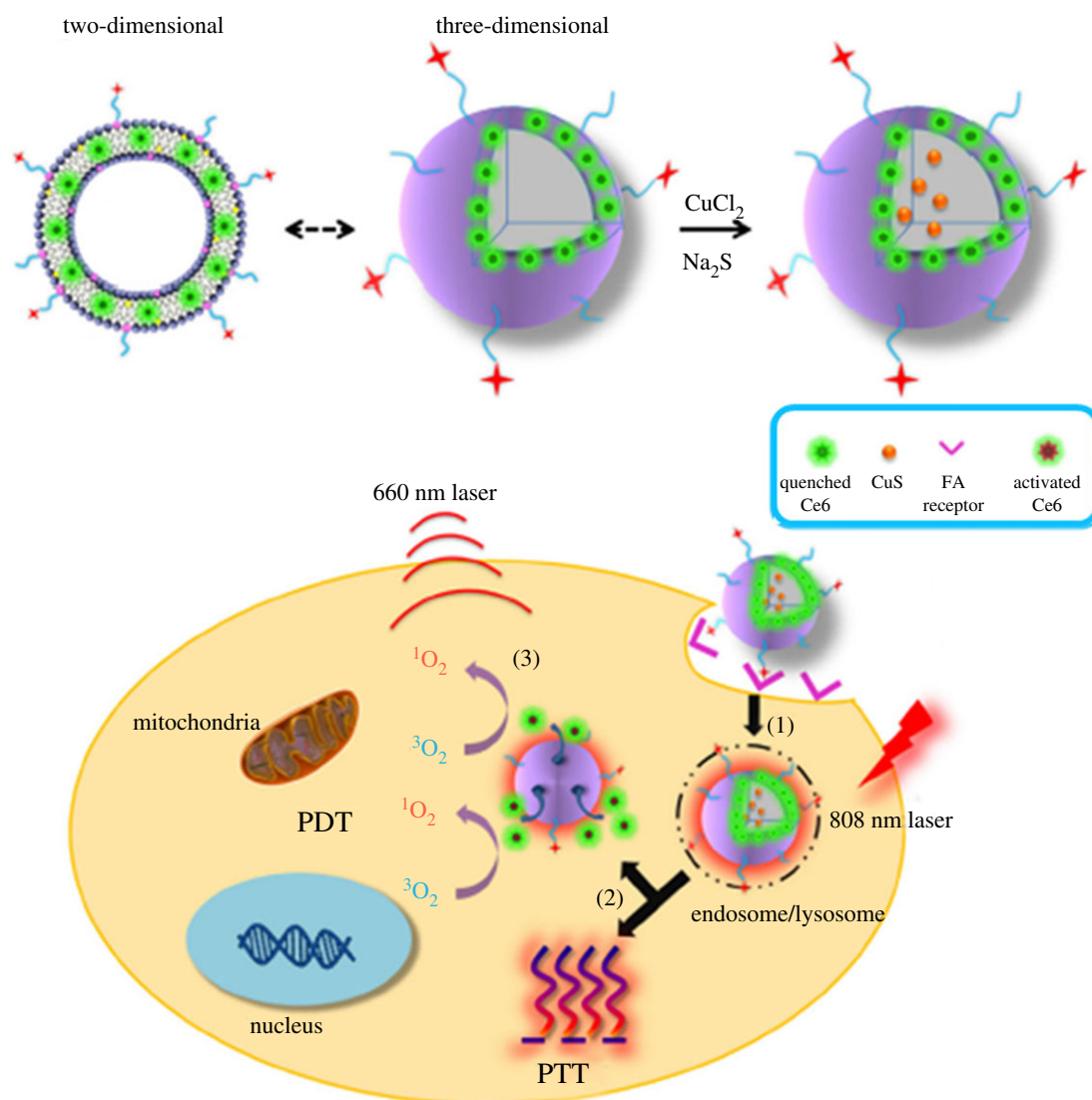


Figure 10. Schematic of thermosensitive liposome encapsulating Ce6 and CuS and its working mechanism; (1) targeting delivery and cell uptake, (2) 808 nm NIR laser-induced PTT effect and PTT-induced Ce6 release and (3) 660 nm laser-induced PDT effect. Adapted from [132].

3.3.2. Multitherapeutic liposomes

3.3.2.1. Emergent cancer treatments

As previously mentioned, the synergistic effect of more than one therapy can greatly improve the efficacy of the cancer defeat. Beside the conventional methods such as chemotherapy, other novel techniques have been using for the treatment of tumours. Among these, magnetic hyperthermia, photodynamic therapy (PDT) or immunotherapy have been rapidly emerging due to their high therapeutic potential.

Hyperthermia is an emergent and particularly attractive strategy based on heat generation by MNPs on the tumour site presenting fewer side effects compared with chemo- and radiotherapy and that can be used in combination with all conventional therapeutic treatments. The mechanism of hyperthermia relies on selective tumoural cell heating (in the temperature range of 41–46°C) resulting in the activation of natural intracellular and extracellular degradation mechanisms that finally lead to apoptosis with cancer cell death [123,124].

PDT is another modality that in the last decades was surprisingly developed in cancer treatment. This is a clinically approved therapeutic modality based on photo-oxidation of biological materials induced by photosensitizers

(PSs) (localized selectively in certain cells or tumoural tissues) activated by a light with appropriate wavelength and in sufficient doses upon irradiation. The activated PS transfers its excited-state energy to surrounding oxygen, resulting in reactive oxygen species, such as singlet oxygen or free radicals, finally causing tumoural cell death with minimal healthy tissue damage [125–127].

Recently, the interest in cancer immunotherapy that stimulates the immune system cells to fight the disease and pursues an opposite strategy with respect to conventional treatments is gaining tremendous interest. This therapeutic strategy does not affect tumoural cells directly, but it activates patient T lymphocytes becoming able to destroy the tumour. Immunotherapy can be obtained by different approaches: cytokines, tumour antigen-targeted monoclonal antibodies, immunological checkpoint inhibitors and therapeutic cancer vaccines. Each of these treatment types has a distinct mechanism of action; however, they all are designed to boost or restore immune function in some manner [107,128–130].

3.3.2.2. Application of liposome as multiactive systems

As clearly stated above, liposomes are very suitable nanocarriers to be employed as multitherapeutic systems.

For example, Pradhan *et al.* [131] developed thermo-sensitive magnetic liposomes using MNPs for hyperthermia-triggered drug release. Liposomes based on thermosensitive PEG were prepared encapsulating IONPs and doxorubicin. Folic acid was conjugated on the surface as targeting molecules for their affinity with folate receptors present on cancer cells. The nanosystems were directed to cancer cells for the presence of a permanent magnetic field, and after internalization an alternating magnetic field was applied to induce MNP heating useful for MNPs and drug release as well as for magnetic hyperthermia. Hence, hyperthermia and chemotherapy treatments were simultaneously promoted and a synergistic effect between the two therapies was observed [131]. Similar thermosensitive liposomes have been prepared to combine photothermal therapy (PTT) and PDT [132]. PTT is nowadays attracting attention due to the possibility of controlling the incorporation of light-activated heating nanoparticles into tumours with consequent high heat deposition in the tumour area at low laser intensities, minimizing the damage in the surrounding healthy tissue [133,134].

In more detail, a photosensitizer (Ce6) was incorporated in the lipid bilayer and copper sulfide (CuS) was encapsulated into the aqueous compartment of the liposome [132]. After the targeted delivery of the photosensitizer into the cancer cells, CuS was activated by laser irradiation inducing PTT-mediated cell killing and at the same time degradation of the liposome. The released Ce6 performed PDT obtaining a synergistic effect with PTT to kill tumour cells (figure 10).

PDT was also associated with chemotherapy to obtain more effective combinations against cancer in the clinic. For example, a novel PEGylated liposome system, named DAFO-DIL incorporating doxorubicin and 5-fluorouracil, was developed by Camacho *et al.* [135]. This nanosystem offered superior therapeutic efficacies compared with free drug administrations and less cytotoxicity. The synergistic effect led to a high reduction (90%) in the tumour growth of murine 4T1 mammary carcinoma *in vivo* [135]. Example of immunotherapy combined with PDT was reported by Mir *et al.* [136]. A photo-immuno-conjugate-associating liposome incorporating the photosensitizer benzoporphyrin derivative monoacid A and the FDA-approved Cetuximab antibody for epidermal growth factor receptor (EGFR) was prepared. By means of this engineered nanosystem, the inhibition of EGFR signalling enhanced PDT-mediated ovarian cancer cell death and the overall synergistic and preferential phototoxicity in an ovarian cancer cell model *in vitro* [136].

In this line, Meraz *et al.* [137] prepared cationic liposomes containing monophosphoryl lipid A (MPL) and interleukin (IL)-12 to demonstrate that the intratumoural administration produced a regression of breast tumour and a systemic immune response. Cationic liposomes have inherent cytotoxicity and the presence of MPL allows recruiting and activation of immune cells besides the cytokine release supporting

tumour regression. To improve the immune response, the IL-12 was added to the MPL liposome. Combined therapy of the liposome incorporating MPL and IL-12 was superior to the activity of any single inhibiting agent and—thanks to the intratumoural administration—tumour growth (4T1 mouse model of breast cancer) was completely blocked. This combined liposomal therapy was able to induce similar reductions in tumour growth in both treated and distal tumours, suggesting a systemic immune response [137].

4. Conclusion

In this review, we discussed recent advances concerning the preparation and application of different multifunctional nanocarriers as molecular imaging-based theranostics. The achieved development in nanomaterial-based combination of therapy and multimodal imaging here reported have shown several unique features that are untenable in traditional medicine. Moreover, the approach of using nanomaterials for specific targeting, molecular imaging and selective therapy has been shown to be both general as well as versatile. This rapidly evolving discipline demonstrates possessing potential to play key roles in every aspect of clinical practice, including early disease detection, diagnosis, staging, personalized treatment, treatment monitoring and follow-up. Those synergistic ‘multiple-in-one’ modalities make personalized and integrated therapy feasible and extremely promising.

Nevertheless, in order to ensure confidence in translating nanomaterials into clinical applications and achieve their definitive utilization, several crucial aspects must be still addressed. Firstly, standard synthetic protocols, measurements and techniques which are necessary for producing and defining a nanoparticle system and for quality control must be unequivocally defined (nanoparticle metrology). Furthermore, nanotoxicity (size-dependent toxicity is one of the most critical issues) and nanomaterial metabolism (the *in vivo* metabolic pathway of nanomaterials) are still not fully biologically understood.

To this scope, we consider that a much stronger involvement of cross-disciplinary researchers (i.e. biologists, pathologists, chemists, material scientists, physicians and engineers) will undoubtedly address these challenges and finally grant the definitive clinical application of nanomedicine.

Competing interests. We declare we have no competing interests.

Funding. The CNIC is supported by the Spanish Ministry of Economy and Competitiveness (MINECO) and the Pro CNIC Foundation and by Severo Ochoa Center of Excellence (MINECO award SEV-2015-0505). We also thank MINECO for grant MAT2013-47303-P, SAF2016-79593-P and for the research grant no. SAF2014-59118-JIN (‘Proyectos de I+D+i para jóvenes investigadores’, 2014) also co-funded by Fondo Europeo de Desarrollo Regional (FEDER).

References

- Schork NJ. 2015 Personalized medicine: time for one-person trials. *Nature* **520**, 609–611. (doi:10.1038/520609a)
- Wistuba II, Gelovani JG, Jacoby JJ, Davis SE, Herbst RS. 2011 Methodological and practical challenges for personalized cancer therapies. *Nat. Rev. Clin. Oncol.* **8**, 135–141. (doi:10.1038/nrdclinonc.2011.2)
- Chan IS, Ginsburg GS. 2011 Personalized medicine: progress and promise. *Annu. Rev. Genomics Hum. Genet.* **12**, 217–244. (doi:10.1146/annurev-genom-082410-101446)
- Kircher MF, Hricak H, Larson SM. 2012 Molecular imaging for personalized cancer care. *Mol. Oncol.* **6**, 182–195. (doi:10.1016/j.molonc.2012.02.005)

5. Willmann JK, van Bruggen N, Dinkelborg LM, Gambhir SS. 2008 Molecular imaging in drug development. *Nat. Rev. Drug Discov.* **7**, 591–607. (doi:10.1038/nrd2290)
6. Peer D, Karp JM, Hong S, Farokhzad OC, Margalit R, Langer R. 2007 Nanocarriers as an emerging platform for cancer therapy. *Nat. Nanotechnol.* **2**, 751–760. (doi:10.1038/nnano.2007.387)
7. Moghimi SM, Hunter AC, Murray JC. 2005 Nanomedicine: current status and future prospects. *FASEB J.* **19**, 311–330. (doi:10.1096/fj.04-2747rev)
8. Lee DE, Koo H, Sun IC, Ryu JH, Kim K, Kwon IC. 2012 Multifunctional nanoparticles for multimodal imaging and theragnosis. *Chem. Soc. Rev.* **41**, 2656–2672. (doi:10.1039/c2cs15261d)
9. Huang Y, He S, Cao W, Cai K, Liang XJ. 2012 Biomedical nanomaterials for imaging-guided cancer therapy. *Nanoscale* **4**, 6135–6149. (doi:10.1039/c2nr31715j)
10. Lee SY, Jeon SI, Jung S, Chung IJ, Ahn CH. 2014 Targeted multimodal imaging modalities. *Adv. Drug Deliv. Rev.* **76**, 60–78. (doi:10.1016/j.addr.2014.07.009)
11. Shin TH, Choi Y, Kim S, Cheon J. 2015 Recent advances in magnetic nanoparticle-based multimodal imaging. *Chem. Soc. Rev.* **44**, 4501–4516. (doi:10.1039/c4cs00345d)
12. Nazir S, Hussain T, Ayub A, Rashid U, MacRobert AJ. 2014 Nanomaterials in combating cancer: therapeutic applications and developments. *Nanomedicine* **10**, 19–34. (doi:10.1016/j.nano.2013.07.001)
13. Lee N, Yoo D, Ling D, Cho MH, Hyeon T, Cheon J. 2015 Iron oxide based nanoparticles for multimodal imaging and magnetoresponsive therapy. *Chem. Rev.* **115**, 10 637–10 689. (doi:10.1021/acs.chemrev.5b00112)
14. Sharma P, Allison JP. 2015 Immune checkpoint targeting in cancer therapy: toward combination strategies with curative potential. *Cell* **161**, 205–214. (doi:10.1016/j.cell.2015.03.030)
15. Castellano JM, Bueno H, Fuster V. 2015 The cardiovascular polypill: clinical data and ongoing studies. *Int. J. Cardiol.* **201**, S8–S14. (doi:10.1016/s0167-5273(15)31027-5)
16. Lonn E, Bosch J, Teo KK, Pais P, Xavier D, Yusuf S. 2010 The polypill in the prevention of cardiovascular diseases: key concepts, current status, challenges, and future directions. *Circulation* **122**, 2078–2088. (doi:10.1161/CIRCULATIONAHA.109.873232)
17. Hu C-MJ, Aryal S, Zhang L. 2010 Nanoparticle-assisted combination therapies for effective cancer treatment. *Ther. Deliv.* **1**, 323–334. (doi:10.4155/tde.10.13)
18. Talelli M, Aires A, Marciello M. 2016 Protein-modified magnetic nanoparticles for biomedical applications. *Curr. Org. Chem.* **20**, 1252–1261. (doi:10.2174/1385272819666150810221009)
19. Marciello M, Connord V, Veintemillas-Verdaguer S, Vergés MA, Carrey J, Respaud M, Serna CJ, Morales MP. 2013 Large scale production of biocompatible magnetite nanocrystals with high saturation magnetization values through green aqueous synthesis. *J. Mat. Chem. B* **1**, 5995–6004. (doi:10.1039/c3tb20949k)
20. Etheridge ML, Campbell SA, Erdman AG, Haynes CL, Wolf SM, McCullough J. 2013 The big picture on nanomedicine: the state of investigational and approved nanomedicine products. *Nanomedicine* **9**, 1–14. (doi:10.1016/j.nano.2012.05.013)
21. Kranz LM *et al.* 2016 Systemic RNA delivery to dendritic cells exploits antiviral defence for cancer immunotherapy. *Nature* **534**, 396–401. (doi:10.1038/nature18300)
22. Yang X *et al.* 2011 CRGD-functionalized, DOX-conjugated, and ⁶⁴Cu-labeled superparamagnetic iron oxide nanoparticles for targeted anticancer drug delivery and PET/MR imaging. *Biomaterials* **32**, 4151–4160. (doi:10.1016/j.biomaterials.2011.02.006)
23. Bouziotis P, Psimadas D, Tsotakos T, Stamopoulos D, Tsoukalas C. 2012 Radiolabeled iron oxide nanoparticles as dual-modality SPECT/MRI and PET/MRI agents. *Curr. Top. Med. Chem.* **12**, 1–9. (doi:10.2174/1568026611212230007)
24. Schlachter EK *et al.* 2011 Metabolic pathway and distribution of superparamagnetic iron oxide nanoparticles: in vivo study. *Int. J. Nanomed.* **6**, 1793–1800. (doi:10.2147/IJN.S23638)
25. Zhang XD *et al.* 2011 Size-dependent in vivo toxicity of PEG-coated gold nanoparticles. *Int. J. Nanomed.* **6**, 2071–2081. (doi:10.2147/IJN.S21657)
26. Hong H, Chen F, Cai W. 2013 Pharmacokinetic issues of imaging with nanoparticles: focusing on carbon nanotubes and quantum dots. *Mol. Imaging Biol.* **15**, 507–520. (doi:10.1007/s11307-013-0648-5)
27. Glaus C, Rossin R, Welch MJ, Bao G. 2010 In vivo evaluation of ⁶⁴Cu-labeled magnetic nanoparticles as a dual-modality PET/MR imaging agent. *Bioconjug. Chem.* **21**, 715–722. (doi:10.1021/bc900511j)
28. Cai W, Chen K, Li Z-B, Gambhir SS, Chen X. 2007 Dual-function probe for PET and near-infrared fluorescence imaging of tumor vasculature. *J. Nucl. Med.* **48**, 1862–1870. (doi:10.2967/jnumed.107.043216)
29. Zhang R, Lu W, Wen X, Huang M, Zhou M, Liang D, Li C. 2011 Annexin A5-conjugated polymeric micelles for dual SPECT and optical detection of apoptosis. *J. Nucl. Med.* **52**, 958–964. (doi:10.2967/jnumed.110.083220)
30. Choi J-S *et al.* 2008 A hybrid nanoparticle probe for dual-modality positron emission tomography and magnetic resonance imaging. *Angew. Chem. Int. Ed.* **47**, 6259–6262. (doi:10.1002/anie.200801369)
31. Däpp S, Müller C, Garayoa E, Bläuenstein P, Maes V, Brans L, Tourwé, DA, Schibli R. 2012 PEGylation, increasing specific activity and multiple dosing as strategies to improve the risk-benefit profile of targeted radionuclide therapy with ¹⁷⁷Lu-DOTA-bombesin analogues. *EJNMMI Res.* **2**, 24. (doi:10.1186/2191-219X-2-24)
32. Däpp S, Garayoa EG, Maes V, Brans L, Tourwé DA, Müller C, Schibli R. 2011 PEGylation of ^{99m}Tc-labeled bombesin analogues improves their pharmacokinetic properties. *Nucl. Med. Biol.* **38**, 997–1009. (doi:10.1016/j.nucmedbio.2011.02.014)
33. de Barros A, Tsourkas A, Saboury B, Cardoso V, Alavi A. 2012 Emerging role of radiolabeled nanoparticles as an effective diagnostic technique. *EJNMMI Res.* **2**, 39. (doi:10.1186/2191-219X-2-39)
34. Hong H, Zhang Y, Sun J, Cai W. 2009 Molecular imaging and therapy of cancer with radiolabeled nanoparticles. *Nano Today* **4**, 399–413. (doi:10.1016/j.nantod.2009.07.001)
35. Thorek DLJ, Chen AK, Czupryna J, Tsourkas A. 2006 Superparamagnetic iron oxide nanoparticle probes for molecular imaging. *Ann. Biomed. Eng.* **34**, 23–38. (doi:10.1007/s10439-005-9002-7)
36. Beyer T *et al.* 2000 A combined PET/CT scanner for clinical oncology. *J. Nucl. Med.* **41**, 1369–1380.
37. Lee N, Hyeon T. 2012 Designed synthesis of uniformly sized iron oxide nanoparticles for efficient magnetic resonance imaging contrast agents. *Chem. Soc. Rev.* **41**, 2575–2589. (doi:10.1039/C1CS15248C)
38. Zhao Z *et al.* 2013 Octapod iron oxide nanoparticles as high-performance T₂ contrast agents for magnetic resonance imaging. *Nat. Commun.* **4**, 2266. (doi:10.1038/ncomms3266)
39. Xiao N, Gu W, Wang H, Deng Y, Shi X, Ye L. 2014 T₁–T₂ dual-modal MRI of brain gliomas using PEGylated Gd-doped iron oxide nanoparticles. *J. Colloid Interface Sci.* **417**, 159–165. (doi:10.1016/j.jcis.2013.11.020)
40. Lin C, Cai S, Feng J. 2012 Positive contrast imaging of SPIO nanoparticles. *J. Nanomater.* **2012**, 1–9. (doi:10.1155/2012/734842)
41. Zahraei M *et al.* 2016 Versatile theranostics agents designed by coating ferrite nanoparticles with biocompatible polymers. *Nanotechnology* **27**, 25 5702–25 5714. (doi:10.1088/0957-4484/27/25/255702)
42. Bhavesh R, Lechuga-Vieco AV, Ruiz-Cabello J, Herranz F. 2015 T₁-MRI fluorescent iron oxide nanoparticles by microwave assisted synthesis. *Nanomaterials* **5**, 1880–1890. (doi:10.3390/nano5041880)
43. Zhou Z *et al.* 2013 Engineered iron-oxide-based nanoparticles as enhanced T₁ contrast agents for efficient tumor imaging. *ACS Nano* **7**, 3287–3296. (doi:10.1021/nn305991e)
44. Valk PE, Delbeke D, Bailey DL, Townsend DW, Maisey MN. 2010 *Positron emission tomography: clinical practice*. London, UK: Springer-Verlag. (doi:10.1007/1-84628-187-3)
45. Fani M, André JP, Maecke H. 2008 ⁶⁸Ga-PET: a powerful generator-based alternative to cyclotron-based PET radiopharmaceuticals. *Contrast Media Mol. Imaging* **3**, 53–60. (doi:10.1002/cmmi.232)
46. Velikyan I. 2015 ⁶⁸Ga-based radiopharmaceuticals: production and application relationship. *Molecules (Basel, Switzerland)* **20**, 12 913–12 943. (doi:10.3390/molecules200712913)
47. Breeman WAP, de Blois E, Sze Chan H, Konijnenberg M, Kwekkeboom DJ, Krenning EP. 2011 ⁶⁸Ga-labeled DOTA-peptides and ⁶⁸Ga labeled

- radiopharmaceuticals for positron emission tomography: current status of research, clinical applications, and future perspectives. *Semin. Nucl. Med.* **41**, 314–321. (doi:10.1053/j.semnucmed.2011.02.001)
48. Poeppel TD, Binse I, Petersenn S, Lahner H, Schott M, Antoch G, Brandau W, Bockisch A, Boy C. 2013 Differential uptake of ^{68}Ga -DOTATOC and ^{68}Ga -DOTATATE in PET/CT of gastroenteropancreatic neuroendocrine tumors. In *Recent Results Cancer Res.* **194**, 353–371. (doi:10.1007/978-3-642-27994-2_18)
49. Kulkarni HR, Baum RP. 2014 Patient selection for personalized peptide receptor radionuclide therapy using Ga-68 somatostatin receptor PET/CT. *PET Clin.* **9**, 83–90. (doi:10.1016/j.cpet.2013.08.015)
50. Poeppel TD, Binse I, Petersenn S, Lahner H, Schott M, Antoch G, Brandau W, Bockisch A, Boy C. 2011 ^{68}Ga -DOTATOC versus ^{68}Ga -DOTATATE PET/CT in functional imaging of neuroendocrine tumors. *J. Nucl. Med.* **52**, 1864–1870. (doi:10.2967/jnumed.111.091165)
51. Rotello V. 2004 *Nanoparticles*. Berlin, Germany: Springer Science+Business Media.
52. Biener J, Wittstock A, Baumann TF, Weissmüller J, Bäumer M, Hamza AV. 2009 Surface chemistry in nanoscale materials. *Materials* **2**, 2404–2428. (doi:10.3390/ma2042404)
53. Chen F *et al.* 2013 Chelator-free synthesis of a dual-modality PET/MRI agent. *Angew. Chem. Int. Ed.* **52**, 13 319–13 323. (doi:10.1002/anie.201306306)
54. Morin G, Wang Y, Ona-Nguema G, Juillot F, Calas G, Menguy N, Aubry E, Bargar JR, Brown GE. 2009 EXAFS and HRTEM evidence for As(III)-containing surface precipitates on nanocrystalline magnetite: implications for As sequestration. *Langmuir* **25**, 9119–9128. (doi:10.1021/la900655v)
55. Chakravarty R, Shukla R, Ram R, Tyagi AK, Dash A, Venkatesh M. 2011 Development of a nano-zirconia based $^{68}\text{Ge}/^{68}\text{Ga}$ generator for biomedical applications. *Nucl. Med. Biol.* **38**, 575–583. (doi:10.1016/j.nucmedbio.2010.10.007)
56. de Blois E, Sze Chan H, Naidoo C, Prince D, Krenning EP, Breeman WAP. 2011 Characteristics of SnO_2 -based $^{68}\text{Ge}/^{68}\text{Ga}$ generator and aspects of radiolabelling DOTA-peptides. *Appl. Radiat. Isot.* **69**, 308–315. (doi:10.1016/j.apradiso.2010.11.015)
57. Chakravarty R, Valdovinos HF, Chen F, Lewis CM, Ellison PA, Luo H, Meyerand ME, Nickles RJ, Cai W. 2014 Intrinsically germanium-69-labeled iron oxide nanoparticles: synthesis and in-vivo dual-modality PET/MR imaging. *Adv. Mater.* **26**, 5119–5123. (doi:10.1002/adma.201401372)
58. Kim DK, Zhang Y, Voit W, Rao KV, Muhammed M. 2001 Synthesis and characterization of surfactant-coated superparamagnetic monodispersed iron oxide nanoparticles. *J. Magn. Magn. Mater.* **225**, 30–36. (doi:10.1016/S0304-8853(00)01224-5)
59. Sun S, Zeng H. 2002 Size-controlled synthesis of magnetite nanoparticles. *J. Am. Chem. Soc.* **124**, 8204–8205. (doi:10.1021/ja026501x)
60. Liao X, Zhu J, Zhong W, Chen HY. 2001 Synthesis of amorphous Fe_2O_3 nanoparticles by microwave irradiation. *Mater. Lett.* **50**, 341–346. (doi:10.1016/S0167-577X(01)00251-8)
61. Wang W-W, Zhu Y-J, Ruan M-L. 2007 Microwave-assisted synthesis and magnetic property of magnetite and hematite nanoparticles. *J. Nanoparticle Res.* **9**, 419–426. (doi:10.1007/s11051-005-9051-8)
62. Pellico J, Lechuga-Vieco AV, Benito M, García-Segura JM, Fuster V, Ruiz-Cabello J, Herranz F. 2015 Microwave-driven synthesis of bisphosphonate nanoparticles allows *in vivo* visualisation of atherosclerotic plaque. *RSC Adv.* **5**, 1661–1665. (doi:10.1039/C4RA13824D)
63. Wong RM, Gilbert DA, Liu K, Louie AY. 2012 Rapid size-controlled synthesis of dextran-coated, ^{64}Cu -doped iron oxide nanoparticles. *ACS Nano* **6**, 3461–3467. (doi:10.1021/nn300494k)
64. Pellico J *et al.* 2016 Fast synthesis and bioconjugation of ^{68}Ga core-doped extremely small iron oxide nanoparticles for PET/MR imaging. *Contrast Media Mol. Imaging* **11**, 203–210. (doi:10.1002/cmmi.1681)
65. Xing Y, Zhao J, Conti PS, Chen K. 2014 Radiolabeled nanoparticles for multimodality tumor imaging. *Theranostics* **4**, 290–306. (doi:10.7150/thno.7341)
66. Prasad PN. 2012 *Introduction to nanomedicine and nanobiotechnology*. New York, NY: Wiley.
67. Enrique M-A, Mariana O-R, Mirshojaei SF, Ahmadi A. 2015 Multifunctional radiolabeled nanoparticles: strategies and novel classification of radiopharmaceuticals for cancer treatment. *J. Drug Target* **23**, 191–201. (doi:10.3109/1061186X.2014.988216)
68. Cai W, Chen X. 2007 Nanoplatforams for targeted molecular imaging in living subjects. *Small* **3**, 1840–1854. (doi:10.1002/sml.200700351)
69. Rudolph C, Gleich B, Flemmer AW. 2010 Cancer nanotechnology. *Methods Mol. Biol. (Clifton NJ)* **624**, 267–280. (doi:10.1007/978-1-60761-609-2)
70. Cuenca AG, Jiang H, Hochwald SN, Delano M, Cance WG, Grobmyer SR. 2006 Emerging implications of nanotechnology on cancer diagnostics and therapeutics. *Cancer* **107**, 459–466. (doi:10.1002/cncr.22035)
71. Chakravarty R, Hong H, Cai W. 2014 Positron emission tomography image-guided drug delivery: current status and future perspectives. *Mol. Pharm.* **11**, 3777–3797. (doi:10.1021/mp500173s)
72. Lee H-Y, Li Z, Chen K, Hsu AR, Xu C, Xie J, Sun S, Chen X. 2008 PET/MRI dual-modality tumor imaging using arginine-glycine-aspartic (RGD)-conjugated radiolabeled iron oxide nanoparticles. *J. Nucl. Med.* **49**, 1371–1379. (doi:10.2967/jnumed.108.051243)
73. Aryal S, Key J, Stigliano C, Landis MD, Lee DY, Decuzzi P. 2014 Positron emitting magnetic nanoconstructs for PET/MR imaging. *Small* **10**, 2688–2696. (doi:10.1002/sml.201303933)
74. Yang BY, Moon S-H, Seelam SR, Jeon MJ, Lee Y-S, Lee DS, Chung J-K, Kim YI, Jeong JM. 2015 Development of a multimodal imaging probe by encapsulating iron oxide nanoparticles with functionalized amphiphiles for lymph node imaging. *Nanomedicine* **10**, 1899–1910. (doi:10.2217/nnm.15.41)
75. British Heart Foundation. Cardiovascular disease. See <https://www.bhf.org.uk/heart-health/conditions/cardiovascular-disease>.
76. Sanz J, Fayad ZA. 2008 Imaging of atherosclerotic cardiovascular disease. *Nature* **451**, 953–957. (doi:10.1038/nature06803)
77. Jaffer FA, Libby P, Weissleder R. 2007 Molecular imaging of cardiovascular disease. *Circulation* **116**, 1052–1061. (doi:10.1161/CIRCULATIONAHA.106.647164)
78. Stendahl JC, Sinusas AJ. 2015 Nanoparticles for cardiovascular imaging and therapeutic delivery, part 2: radiolabeled probes. *J. Nucl. Med.* **56**, 1637–1641. (doi:10.2967/jnumed.115.164145)
79. Lukyanov AN, Hartner WC, Torchilin VP. 2004 Increased accumulation of PEG-PE micelles in the area of experimental myocardial infarction in rabbits. *J. Control Release* **94**, 187–193. (doi:10.1016/j.jconrel.2003.10.008)
80. Majmudar MD *et al.* 2013 Polymeric nanoparticle PET/MR imaging allows macrophage detection in atherosclerotic plaques. *Circ. Res.* **112**, 755–761. (doi:10.1161/CIRCRESAHA.111.300576)
81. Seo JW, Baek H, Mahakian LM, Kusunose J, Hamzaj J, Ruoslahti E, Ferrara KW. 2014 ^{64}Cu -labeled LyP-1-dendrimer for PET-CT imaging of atherosclerotic plaque. *Bioconjug. Chem.* **25**, 231–239. (doi:10.1021/bc400347s)
82. Luehmann HP, Pressly ED, Detering L, Wang C, Pierce R, Woodard PK, Gropler RJ, Hawker CJ, Liu Y. 2014 PET/CT imaging of chemokine receptor CCR5 in vascular injury model using targeted nanoparticle. *J. Nucl. Med.* **55**, 629–634. (doi:10.2967/jnumed.113.132001)
83. Nahrendorf M, Keliher E, Marinelli B, Leuschner F, Robbins CS, Gerszten RE, Pittet MJ, Swirski FK, Weissleder R. 2011 Detection of macrophages in aortic aneurysms by nanoparticle positron emission tomography-computed tomography. *Arterioscler. Thromb. Vasc. Biol.* **31**, 750–757. (doi:10.1161/ATVBAHA.110.221499)
84. Ueno T *et al.* 2013 Nanoparticle PET-CT detects rejection and immunomodulation in cardiac allografts. *Circulation* **6**, 568–573. (doi:10.1161/CIRCIMAGING.113.000481)
85. Jung C *et al.* 2014 Intraperitoneal injection improves the uptake of nanoparticle-labeled high-density lipoprotein to atherosclerotic plaques compared with intravenous injection: a multimodal imaging study in ApoE knockout mice. *Circulation* **7**, 303–311. (doi:10.1161/CIRCIMAGING.113.000607)
86. Pattni BS, Chupin VV, Torchilin VP. 2015 New developments in liposomal drug delivery. *Chem. Rev.* **115**, 10 938–10 966. (doi:10.1021/acs.chemrev.5b00046)
87. Nogueira E, Gomes AC, Preto A, Cavaco-Paulo A. 2015 Design of liposomal formulations for cell targeting. *Colloid Surf. B* **136**, 514–526. (doi:10.1016/j.colsurfb.2015.09.034)

88. Mura S, Nicolau J, Couvreur P. 2013 Stimuli-responsive nanocarriers for drug delivery. *Nat. Mater.* **12**, 991–1003. (doi:10.1038/NMAT3776)
89. Tila D, Ghasemi S, Yazdani-Arazi SN, Ghanbarzadeh S. 2015 Functional liposomes in the cancer-targeted drug delivery. *J. Biomater. Appl.* **30**, 3–16. (doi:10.1177/0885328215578111)
90. Eloy JO, Claro de Souza M, Petrilli R, Barcellos JPA, Lee RJ, Marchetti JM. 2014 Liposomes as carriers of hydrophilic small molecule drugs: strategies to enhance encapsulation and delivery. *Colloid Surf. B* **123**, 345–363. (10.1016/j.colsurfb.2014.09.029)
91. Bochicchio S, Dalmoro A, Barba AA, Grassi G, Lamberti G. 2014 Liposomes as siRNA delivery vectors. *Curr. Drug Metab.* **15**, 882–892. (doi:10.2174/1389200216666150206124913)
92. Mallick S, Choi JS. 2014 Liposomes: versatile and biocompatible nanovesicles for efficient biomolecules delivery. *J. Nanosci. Nanotechnol.* **14**, 755–765. (doi:10.1166/jnn.2014.9080)
93. Du AW, Stenzel MH. 2014 Drug carriers for the delivery of therapeutic peptides. *Biomacromolecules* **15**, 1097–1114. (doi:10.1021/bm500169p)
94. Sharma NK, Kumar V. 2014 Liposomes as triggerable carrier for intracellular drug delivery. *Drug Deliv. Lett.* **4**, 12–20. (doi:10.2174/2210303103999131211109080)
95. Gardikis K, Tsimploulis C, Dimas K, Micha-Screttas M, Demetzos C. 2010 New chimeric advanced drug delivery nano systems (chi-aDDnSs) as doxorubicin carriers. *Int. J. Pharm.* **402**, 231–237. (doi:10.1016/j.ijpharm.2010.10.007)
96. Barenholz Y. 2012 Doxil® – the first FDA-approved nano-drug: lessons learned. *J. Control Release* **160**, 117–134. (doi:10.1016/j.jconrel.2012.03.020)
97. Park JW. 2002 Liposome-based drug delivery in breast cancer treatment. *Breast Cancer Res.* **4**, 95–99. (doi:10.1186/bcr432)
98. Andreopoulou E, Gaiotti D, Kim E, Downey A, Mirchandani D, Hamilton A, Jacobs A, Curtin J, Muggia F. 2007 Pegylated liposomal doxorubicin HCL (PLD; Caelyx/Doxil): experience with long-term maintenance in responding patients with recurrent epithelial ovarian cancer. *Ann. Oncol.* **18**, 716–721. (doi:10.1093/annonc/mdl484)
99. Chou HH *et al.* 2006 Pegylated liposomal doxorubicin (Lipo-Dox) for platinum-resistant or refractory epithelial ovarian carcinoma: a Taiwanese gynecologic oncology group study with long-term follow-up. *Gynecol. Oncol.* **101**, 423–428. (doi:10.1016/j.ygyno.2005.10.027)
100. Silverman JA, Deitcher SR. 2013 Marqibo® (vincristine sulfate liposome injection) improves the pharmacokinetics and pharmacodynamics of vincristine. *Cancer Chemother. Pharmacol.* **71**, 555–564. (doi:10.1007/s00280-012-2042-4)
101. Rivera E. 2003 Liposomal anthracyclines in metastatic breast cancer: clinical update. *Oncologist* **8**(Suppl. 2), 3–9. (doi:10.1634/theoncologist.8-suppl_2-3)
102. D'Acremont V, Herzog C, Genton B. 2006 Immunogenicity and safety of a virosomal hepatitis A vaccine (Epaxal) in the elderly. *J. Travel Med.* **13**, 78–83. (doi:10.1111/j.1708-8305.2006.00001.x)
103. Patil SD, Burgess DJ. 2005 Liposomes, design and manufacturing. In *Injectable dispersed systems: formulation, processing and performance (drugs and the pharmaceutical sciences series)* (ed. DJ Burgess), pp. 249–303. New York, NY: Marcel Dekker. (ISBN 9780849336997)
104. Drugs.com homepage on the Internet. DepoCyt® (cytarabine liposome injection) prescribing information. See <http://www.drugs.com/pro/depocyt.html> (accessed 18 August 2016).
105. Yarmolenko PS, Zhao Y, Landon C, Spasojevic I, Yuan F, Needham D, Viglianti BL, Dewhirst MW. 2010 Comparative effects of thermosensitive doxorubicin-containing liposomes and hyperthermia in human and murine tumours. *Int. J. Hyperthermia* **26**, 485–498. (doi:10.3109/02656731003789284)
106. Farhat FS *et al.* 2011 A phase II study of lipoplatin (liposomal cisplatin)/vinorelbine combination in HER-2/neu-negative metastatic breast cancer. *Clin. Breast Cancer* **11**, 384–389. (doi:10.1016/j.clbc.2011.08.005)
107. Casagrande N, Celegato M, Borghese C, Mongiat M, Colombatti A, Aldinucci D. 2014 Preclinical activity of the liposomal cisplatin lipoplatin in ovarian cancer. *Clin. Cancer Res.* **20**, 5496–5506. (doi:10.1158/1078-0432.CCR-14-0713)
108. Mylonakis N, Athanasiou A, Ziras N, Angel J, Rapti A, Lampaki S, Politis N, Karanikas C, Kosmas C. 2010 Phase II study of liposomal cisplatin (Lipoplatin) plus gemcitabine versus cisplatin plus gemcitabine as first line treatment in inoperable (stage IIIB/IV) nonsmall cell lung cancer. *Lung Cancer* **68**, 240–247. (doi:10.1016/j.lungcan.2009.06.017)
109. Ravaoli A *et al.* 2009 Lipoplatin monotherapy: a phase II trial of second-line treatment of metastatic non-small-cell lung cancer. *J. Chemother.* **21**, 86–90. (doi:10.1179/joc.2009.21.1.86)
110. Stathopoulos GP, Boulikas T. 2012 Lipoplatin formulation review article. *J. Drug Deliv.* **2012**, 581 363–581 373. (doi:10.1155/2012/581363)
111. Bangham A, Gier J, Greville G. 1967 Osmotic properties and water permeability of phospholipid liquid crystals. *Chem. Phys. Lipids* **1**, 225–246. (doi:10.1016/0009-3084(67)90030-8)
112. Szoka Jr F, Papahadjopoulos D. 1978 Procedure for preparation of liposomes with large internal aqueous space and high capture by reverse-phase evaporation. *Proc. Natl Acad. Sci. USA* **75**, 4194–4198. (doi:10.1073/pnas.75.9.4194)
113. Batzri S, Korn ED. 1973 Single bilayer liposomes prepared without sonication. *Biochim. Biophys. Acta* **298**, 1015–1019. (doi:10.1016/0005-2736(73)90408-2)
114. Laouini A, Jaafar-Maalej C, Limayem-Blouza I, Sfar S, Charcosset C, Fessi H. 2012 Preparation, characterization and applications of liposomes: state of the art. *J. Colloid Sci. Biotechnol.* **1**, 147–168. (doi:10.1166/jcsb.2012.1020)
115. Lesoin L, Crampon C, Boutin O, Badens E. 2011 Development of a continuous dense gas process for the production of liposomes. *J. Supercrit. Fluids* **60**, 51–62. (doi:10.1016/j.supflu.2011.04.018)
116. Petersen AL, Hansen AE, Gabizon A, Andresen TL. 2012 Liposome imaging agents in personalized medicine. *Adv. Drug Deliv. Rev.* **64**, 1417–1435. (doi:10.1016/j.addr.2012.09.003)
117. Perche F, Torchilin VP. 2013 Recent trends in multifunctional liposomal nanocarriers for enhanced tumor targeting. *J. Drug Deliv.* **2013**, 1–32. (doi:10.1155/2013/705265)
118. Tagami T, Foltz WD, Ernsting MJ, Lee CM, Tannock IF, May JP, Li S-D. 2011 MRI monitoring of intratumoral drug delivery and prediction of the therapeutic effect with a multifunctional thermosensitive liposome. *Biomaterials* **32**, 6570–6578. (doi:10.1016/j.biomaterials.2011.05.029)
119. De Palma M, Hanahan D. 2012 The biology of personalized cancer medicine: facing individual complexities underlying hallmark capabilities. *Mol. Oncol.* **6**, 111–127. (doi:10.1016/j.molonc.2012.01.011)
120. Ren L, Chen S, Li H, Zhang Z, Zhong J, Liu M, Zhou X. 2016 MRI-guided liposomes for targeted tandem chemotherapy and therapeutic response prediction. *Acta Biomater.* **35**, 260–268. (doi:10.1016/j.actbio.2016.02.011)
121. Rizzitelli S, Giustetto P, Faletto D, Castelli DD, Aime S, Terreno E. 2016 The release of Doxorubicin from liposomes monitored by MRI and triggered by a combination of US stimuli led to a complete tumor regression in a breast cancer mouse model. *J. Control Release* **230**, 57–63. (doi:10.1016/j.jconrel.2016.03.040)
122. Guo H, Chen W, Sun X, Liu Y-N, Li J, Wang J. 2015 Theranostic magnetoliposomes coated by carboxymethyl dextran with controlled release by low-frequency alternating magnetic field. *Carbohydr. Polym.* **118**, 209–217. (doi:10.1016/j.carbpol.2014.10.076)
123. Hilger I, Kaiser WA. 2012 Iron oxide-based nanostructures for MRI and magnetic hyperthermia. *Nanomedicine* **7**, 1443–1459. (doi:10.2217/nmm.12.112)
124. Thiesen B, Jordan A. 2008 Clinical applications of magnetic nanoparticles for hyperthermia. *Int. J. Hypertherm.* **24**, 467–474. (doi:10.1080/02656730802104757)
125. Dolmans DE, Fukumura D, Jain RK. 2003 Photodynamic therapy for cancer. *Nat. Rev. Cancer* **3**, 380–387. (doi:10.1038/nrc1071)
126. Ethirajan M, Chen Y, Joshi P, Pandey RK. 2011 The role of porphyrin chemistry in tumor imaging and photodynamic therapy. *Chem. Soc. Rev.* **40**, 340–362. (doi:10.1039/b915149b)
127. Lim CK *et al.* 2013 Nanophotosensitizers toward advanced photodynamic therapy of cancer. *Cancer Lett.* **334**, 176–187. (doi:10.1016/j.canlet.2012.09.012)
128. Mellman I, Couks G, Dranoff G. 2011 Cancer immunotherapy comes of age. *Nature* **480**, 480–489. (doi:10.1038/nature10673)
129. Galon J *et al.* 2006 Type, density, and location of immune cells within human colorectal tumors

- predict clinical outcome. *Science* **313**, 1960–1964. (doi:10.1126/science.1129139)
130. Dunn GP, Koebel CM, Schreiber RD. 2006 Interferons, immunity and cancer immunoediting. *Nat. Rev. Immunol.* **6**, 836–848. (doi:10.1038/nri1961)
131. Pradhan P, Giri J, Rieken F, Koch C, Mykhaylyk O, Doblinger M, Banerjee R, Bahadur D, Plank C. 2010 Targeted temperature sensitive liposomes for thermo-chemotherapy. *J. Control Release* **42**, 108–121. (doi:10.1016/j.jconrel.2009.10.002)
132. Tan X, Pang X, Lei M, Ma M, Guo F, Wang J, Yu M, Tan F, Li N. 2016 An efficient dual-loaded multifunctional nanocarrier for combined photothermal and photodynamic therapy based on copper sulphide and chlorin e6. *Int. J. Pharm.* **503**, 220–228. (doi:10.1016/j.ijpharm.2016.03.019)
133. Jain PK, Huang X, El-Sayed IH, El-Sayed MA. 2008 Noble metals on the nanoscale: optical and photothermal properties and some applications in imaging, sensing, biology, and medicine. *Acc. Chem. Res.* **41**, 1578–1586. (doi:10.1021/ar7002804)
134. Jaque D, Martínez Maestro L, del Rosal B, Haro-Gonzalez P, Benayas A, Plaza JL, Martín Rodríguez E, García Solé J. 2014 Nanoparticles for photothermal therapies. *Nanoscale* **6**, 9494–9530. (doi:10.1039/c4nr00708e)
135. Camacho KM *et al.* 2016 DAFODIL: a novel liposome-encapsulated synergistic combination of doxorubicin and 5FU for low dose chemotherapy. *J. Control Release* **229**, 154–162. (doi:10.1016/j.jconrel.2016.03.027)
136. Mir Y, Elrington SA, Hasan T. 2013 A new nanoconstruct for epidermal growth factor receptor-targeted photo-immunotherapy of ovarian cancer. *Nanomed. Nanotechnol.* **9**, 1114–1122. (doi:10.1016/j.nano.2013.02.005)
137. Meraz IM, Savage DJ, Segura-Ibarra V, Li J, Rhudy J, Gu J, Serda RE. 2014 Adjuvant cationic liposomes presenting MPL and IL-12 induce cell death, suppress tumor growth, and alter the cellular phenotype of tumors in a murine model of breast cancer. *Mol. Pharm.* **11**, 3484–3491. (doi:10.1021/mp5002697)